Transient apoptosis inhibition in donor stem cells improves hematopoietic stem cell transplantation

Matthias Kollek,[1,3] Gesina Voigt,[1] Christian Molnar,[1,3,4] Fabronia Murad,[7] Daniela Bertele,[1] Christopher Felix Krombholz,[1] Sheila Bohler,[1,3] Verena Labi,[8] Stefan Schiller,[5,6] Mirjam Kunze,[2] Stephan Geley,[9] Charlotte M. Niemeyer,[1] Ana Garcia-Saez,[7] and Miriam Erlacher[1,5]

[1]Division of Pediatric Hematology and Oncology, Department of Pediatrics and Adolescent Medicine and [2]Department of Obstetrics and Gynecology, University Medical Center Freiburg, Faculty of Medicine, University of Freiburg, Freiburg, Germany
[3]Faculty of Biology, [4]Spemann Graduate School of Biology and Medicine, [5]Freiburg Institute for Advanced Studies, and [6]Center for Biological Systems Analysis, University of Freiburg, Freiburg, Germany
[7]Interfaculty Institute of Biochemistry, University of Tübingen, Tübingen, Germany
[8]Division of Developmental Immunology and [9]Division of Molecular Pathophysiology, Biocenter, Medical University of Innsbruck, Innsbruck, Austria

During hematopoietic stem cell transplantation, a substantial number of donor cells are lost because of apoptotic cell death. Transplantation–associated apoptosis is mediated mainly by the proapoptotic BCL-2 family proteins BIM and BMF, and their proapoptotic function is conserved between mouse and human stem and progenitor cells. Permanent inhibition of apoptosis in donor cells caused by the loss of these BH3-only proteins improves transplantation outcome, but recipients might be exposed to increased risk of lymphomagenesis or autoimmunity. Here, we address whether transient inhibition of apoptosis can serve as a safe but efficient alternative to improve the outcome of stem cell transplantation. We show that transient apoptosis inhibition by short-term overexpression of prosurvival BCL-XL, known to block BIM and BMF, is not only sufficient to increase the viability of hematopoietic stem and progenitor cells during engraftment but also improves transplantation outcome without signs of adverse pathologies. Hence, this strategy represents a promising and novel therapeutic approach, particularly under conditions of limited donor stem cell availability.

INTRODUCTION

Hematopoietic stem cell (HSC) transplantation (HSCT) is a curative treatment for many hematological, immunological, and malignant diseases. Graft failure and delayed engraftment can be caused by HLA incompatibility between donor and recipient, decreased fitness, or a low number of stem cells available for transfer (Barrett et al., 2003; Chen et al., 2004; Mattsson et al., 2008; Maie et al., 2014). The risk factors for receiving insufficient numbers of vital cells are manifold and include relevant differences in body weight between patient and donor (Yabe et al., 2014) and umbilical cord blood (UCB) as stem cell source, because a single UCB sample contains a limited number of hematopoietic stem and progenitor cells (HSPCs) that often do not suffice to successfully reconstitute an adult patient (Wagner et al., 2002; Ballen et al., 2013). In the setting of peripheral blood stem cell transplantation, insufficient stem cell numbers might be collected from donors showing limited response to G-CSF treatment (poor mobilizers; Bakanay and Demirer, 2012).

Different approaches to provide higher vital donor stem cell numbers to the recipient are currently being investigated in preclinical studies and clinical trials (Rocha and Broxmeyer, 2010). For poor mobilizers, combined treatment of the donor with G-CSF and the CXCR4 antagonist plerixafor has been shown to efficiently increase the yield of stem cells (Bakanay and Demirer, 2012). To obtain higher cell numbers for UCB transplantation, two grafts can be cotransplanted (Haspel and Ballen, 2006) or HSPCs can be expanded ex vivo before transplantation (Horwitz, 2016). HSPC expansion, however, may come at the cost of reduced stemness, because proliferating HSPCs tend to differentiate and lose their self-renewal potential and long-term repopulating ability (Delaney et al., 2010; de Lima et al., 2012). Currently, the most promising strategy for ex vivo expansion involves the cytokines SCF, FLT3L, TPO, and IL-6 in combination with the aryl hydrocarbon receptor antagonist stemregenin-1 (SR-1; Boitano et al., 2010; Wagner et al., 2016).

We have recently shown that a substantial number of donor HSPCs are lost during transplantation because of apoptotic cell death controlled by BCL-2 family proteins and that the lack of signals derived from the stem cell niche participates

Correspondence to: Miriam Erlacher: miriam.erlacher@uniklinik-freiburg.de

Abbreviations used: CPP, cell-penetrating peptide; HSC, hematopoietic stem cell; HSCT, HSC transplantation; HSPC, hematopoietic stem and progenitor cell; LSK, lineage marker negative, sca-1 positive, cKit positive; LT-HSC, long-term HSC; PTD, protein transduction domain; TAT, protein transduction domain of HIV-TAT protein; UCB, umbilical cord blood.

in this transplantation-associated apoptosis (Labi et al., 2013). Upon harvest or mobilization for HSCT, HSPCs are deprived of critical prosurvival signals, such as cytokines or cell–cell or cell–matrix interactions, and lack of these signals triggers apoptosis. Destruction of stem cell niches by toxic preparative conditioning regimens (e.g., total body irradiation) prolongs the period of decreased survival signals from host tissues, further priming HSPCs for apoptosis (Hooper et al., 2009).

Both cytokine deprivation and detachment from the extracellular matrix induce cell death via the intrinsic apoptosis pathway. Intrinsic apoptosis is regulated by the BCL-2 protein family, which consists of both proapoptotic proteins (e.g., BAX, BAK, BIM, PUMA, and BMF) and antiapoptotic proteins (BCL-2, BCL-XL, MCL-1, A1/BFL, BCL-W; Labi et al., 2006). A tightly regulated interplay between the pro- and antiapoptotic Bcl-2 family members is crucial for the generation, maintenance, and function of the hematopoietic system (Kollek et al., 2016). We have previously identified BIM and BMF as two proapoptotic BCL-2 proteins from the BCL-2 homology domain 3 (BH3)–only subgroup that are decisive for most transplantation-associated apoptosis in mice (Labi et al., 2013). Both proteins have been associated with apoptosis induced by growth factor withdrawal and cell–matrix detachment (Puthalakath et al., 2001; Czabotar et al., 2014). In mouse lineage marker–negative, Sca-1– and c-kit–positive (LSK) cells, a population enriched in HSPCs, both *Bim* and *Bmf* were transcriptionally repressed by the cytokines SCF and Flt3L. In the absence of these cytokines, LSK cells died mainly in a BIM-dependent manner (Labi et al., 2013). During transplantation, lack of either BIM or BMF or over-expression of one of their antagonists, BCL-2 or BCL-XL, resulted in prolonged survival of LSK cells correlating with an increased reconstitution potential as compared with wild type competitor cells. In line, less donor BM cells were required for successful engraftment when BIM was absent. Although BMF-mediated HSPC apoptosis seemed to be relevant specifically during the early engraftment period, BIM was also critical for regulating long-term hematopoiesis. Notably, WT LSK cells were gradually displaced by BIM-deficient cells over time in competitive reconstitution experiments. In vitro and in vivo fitness of human cord blood CD34$^+$ cells, a population enriched in HSPCs, could be significantly improved when BIM or BMF was knocked down individually by lentiviral shRNA, indicating that transplantation-induced apoptosis is governed by conserved pathways between mice and humans (Labi et al., 2013). These data suggested that inhibition of BIM and/or BMF in donor HSPCs could be a useful means to achieve superior transplantation outcome. Permanent apoptosis resistance, however, is associated with an increased risk of leukemogenesis and autoimmunity, and recipient mice transplanted with *Bim*$^{-/-}$ or *Bim*$^{-/-}$*Bmf*$^{-/-}$ BM cells died of autoimmune kidney disease and/or lymphoma within 1 yr (Labi et al., 2014; Woess et al., 2015).

An alternative approach to permanent apoptosis inhibition is to limit apoptosis resistance to a time period relevant for the transplantation procedure. Likely, this strategy would also decrease the risk of undesired side effects. To provide support for this hypothesis, we transiently inhibited BIM and BMF in mouse HSPCs by overexpression of their prosurvival antagonist BCL-XL ex vivo using adenoviral vectors or protein transduction of recombinant full-length BCL-XL. Thereby, we confirm that promoting short-term apoptosis resistance during HSCT is sufficient to improve HSPC performance. At the same time, transient BCL-XL overexpression in donor cells does not cause or accelerate lymphomagenesis in the recipients. Our findings suggest that transient inhibition of apoptosis by donor HSPC manipulation ex vivo increases the fitness of these cells without elevating the risk of adverse pathology. Thus transient apoptosis inhibition represents a promising approach to reduce the risk of graft failure and improve HSCT outcome.

RESULTS

Short-term BCL-XL overexpression transiently protects mouse LSK cells from apoptosis without impairing colony formation

To test whether ectopic but transient inhibition of intrinsic apoptosis would promote HSPC fitness, we chose the antiapoptotic protein BCL-XL because of its high affinity for various proapoptotic BH3-only proteins, particularly BIM and BMF (Chen et al., 2005). For transient gene expression, a replication-defective adenoviral backbone based on the adenovirus serotype 5 (Ad5) and previously shown to efficiently infect mouse LSK cells was used (Bradfute and Goodell, 2003). Adenoviruses do not readily integrate into the host genome but preferentially remain episomal. With every cell division, their copy number is diluted, leading to only transient gene expression in proliferating cells (McConnell and Imperiale, 2004). The human protein BCL-XL (97% identical to the mouse protein; Fang et al., 1994) was overexpressed under control of the CMV promoter (Ad5–BCL-XL) in mouse LSK cells (Fig. 1 A). An adenovirus expressing the fluorescent protein Venus (Ad5-Venus) was used as control. When mouse LSK cells were transfected at a multiplicity of infection of 10, highest Venus expression was observed after 1–3 d with a transduction efficiency of up to 60%. Subsequently, Venus expression gradually declined and disappeared within 7–9 d upon transduction (Fig. 1 B). Adenoviral BCL-XL overexpression was confirmed by Western blot in HeLa cells and by intracellular flow cytometry in LSK cells (Fig. 1 C and Fig. S1 B). Although viral transduction reduced LSK cell viability by ~10% when compared with untreated controls, transiently overexpressed BCL-XL robustly inhibited apoptosis induced by exogenous DNA damage caused by the topoisomerase inhibitor etoposide, confirming functionality of the transgene (Fig. 1 D). In addition, adenoviral BCL-XL overexpression protected LSK cells from cytokine deprivation–induced apoptosis, but the strength of this protective effect decreased over time, in line with transient transgene expression (Fig. 1 E). To exclude effects of adenoviral infection and/or BCL-XL overexpression on differentiation, transduced
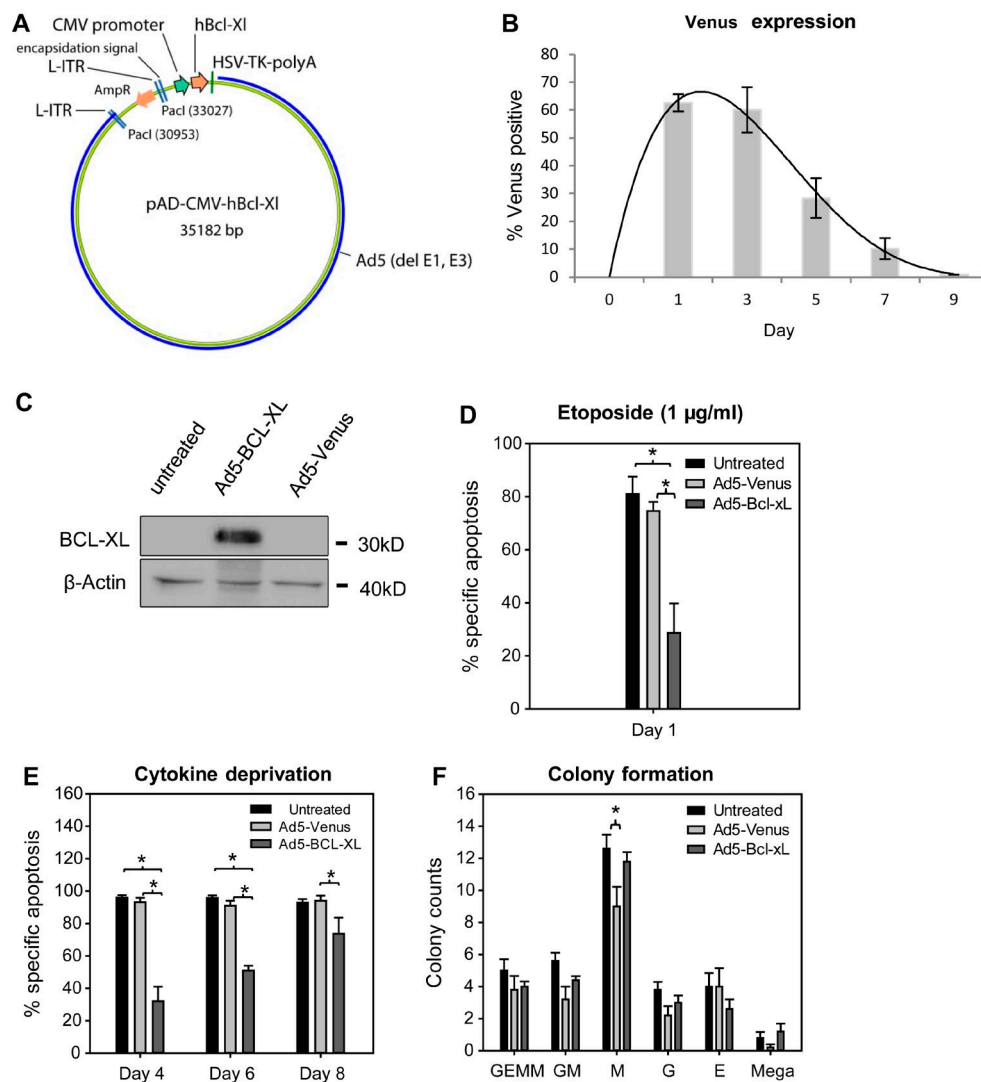
Figure 1. **Adenoviral overexpression of BCL-XL confers short-term protection to LSK cells.** (A) Adenoviral vectors for human BCL-XL expression were used. (B) WT LSK cells were transduced with Ad5-Venus viruses and cultured in the presence of cytokines (SCF, TPO, and Flt3L). Venus expression was determined by flow cytometry at the indicated time points. Bars represent means ± SEM (n = 3 independent experiments). (C) HeLa cells were transduced with the indicated adenoviruses, and BCL-XL protein was determined 48 h later. (D) LSK cells were either left untreated or transduced with the indicated adenoviruses and, at the same time, treated with 1 µg/ml etoposide. After 24 h, apoptosis was determined by flow cytometry. Bars represent means of three to four independent experiments ± SEM (Mann–Whitney test; P = 0.05 untreated vs. Ad5–BCL-XL and Ad5-Venus vs. Ad5–BCL-XL). (E) Adenovirally trans-duced cells were subjected to cytokine withdrawal, and apoptosis was determined by flow cytometry at the indicated time points. Bars represent means of four independent experiments ± SEM (Mann–Whitney test; P = 0.02 for untreated vs. Ad5–BCL-XL and Ad5-Venus vs. Ad5–BCL-XL at day 4 and 6; P = 0.04 for Ad5-Venus vs. Ad5–BCL-XL at day 8). (F) 300 LSK cells were transduced with adenoviruses or left untreated and cultured in MethoCult medium supple-mented with rmSCF, rmIL-3, rhIL-6, and rhEpo. After 7 d, colonies were counted, and the colony type was determined based on morphological features. Bars represent means of n = 4 independent experiments ± SEM (Mann–Whitney test; P = 0.04 for M colonies).

LSK cells were analyzed for their colony-forming potential, but no substantial differences were observed (Fig. 1 F).

Donor stem cells transiently overexpressing BCL-XL display an engraftment advantage that is reflected by long-term chimerism in vivo

To test whether short-term inhibition of apoptosis by BCL-XL is sufficient to improve LSK cell fitness during

transplantation, competitive reconstitution experiments using ex vivo adenovirally transduced LSK cells were per-formed. Ly5.1/Ly5.2 heterozygous recipient mice were le-thally irradiated and reconstituted with a 50:50 mix of LSK cells derived from a Ly5.2[+] donor and an isogenic Ly5.1[+] donor. Whereas the Ly5.2^{+} LSK cells were infected ex vivo either with Ad5-Venus (group 1) or Ad5–BCL-XL (group 2) adenoviruses, Ly5.1[+] competitor LSK cells were invariably

infected with Ad5-Venus viruses (Fig. 2 A) in order to determine the effects of transient apoptosis inhibition that are independent of potential influences of adenoviral infection on HSC function. In addition, we transplanted a third cohort of recipient mice with a 50:50 mix of noninfected Ly5.2$^+$ LSK cells and Ly5.1$^+$ LSK cells infected with Ad5-Venus (group 3) to identify changes in HSC fitness conferred by the adenoviral infection itself. Recipients were sacrificed for analysis 10 d after transplantation. Analysis of recipient mice included LSK and myeloid cells isolated from the BM, thymocytes, and granulocytes and monocytes from the spleen (Fig. 2, B–D; and Fig. S2 A). Mature lymphocytes were excluded from the analysis because they were still entirely derived from the recipient mice at the time of analysis. As expected, no competitive advantage of Ly5.2$^+$ donor cells was observed when both donor samples were transduced with Ad5-Venus (group 1). In contrast, Ly5.2$^+$ LSK cells transiently overexpressing BCL-XL showed a strongly increased engraftment as reflected by displacement of Ly5.1$^+$ cells (group 2). This indicates that apoptosis-resistant LSK cells had a robust competitive advantage during transplantation. The higher number of Ly5.2$^+$ granulocytes and monocytes in the BM of group 2 recipient mice compared with group 1 mice reflects a faster onset of blood formation (Fig. S2 A). However, a strong predominance of Ly5.2$^+$ cells over Ly5.1$^+$ cells was observed in group 3 recipient mice, indicating that the adenoviral infection of HSPCs ex vivo resulted in a substantial loss in competitiveness in vivo, a result that was not anticipated from the colony-forming assays described above (Fig. 1 F). To determine whether adenoviral infection by itself is toxic in a cell-intrinsic manner or whether infected and/or Venus–overexpressing cells are eliminated by recipient T cells, competitive reconstitution experiments were performed using T cell–deficient Ly5.2$^+$ Rag1$^{-/-}$ recipients. As described previously, engraftment of Ly5.1$^+$ cells in Ly5.2$^+$ recipients was generally low (Waterstrat et al., 2010). However, despite the absence of T cells, Ad5-Venus–infected LSK cells performed significantly worse than noninfected counterparts, indicating cell-intrinsic toxicity of adenoviral infection in mouse HSPCs as the major cause of poor engraftment (Fig. S2 B).

Because apoptosis inhibition in our system is restricted to the first days after transplantation, the chimerism at day 10 should be stably transmitted to later time points. Indeed, analysis of recipient mice of all experimental groups 16 wk after transplantation showed an overall similar Ly5.1$^+$/Ly5.2$^+$ chimerism as compared with the day 10 analysis (Fig. 2, E–G; and Table 1). This indicates that adenoviral BCL-XL overexpression conferred sufficient protection to long-term HSCs (LT-HSCs), the cells that maintain long-term hematopoiesis (Purton and Scadden, 2007). At this late time point, BM chimerism was also reflected by the Ly5.1$^+$/Ly5.2$^+$ chimerism of lymphocytes (Fig. 2 F). Importantly, Ly5.2$^+$ LSK cells transduced with Ad5–BCL-XL completely outcompeted untreated Ly5.1$^+$ LSK cells in a competitive setting, indicating that transient BCL-XL overexpression was able to protect

mouse HSPCs from both virus-induced and transplantation-associated apoptosis (Fig. S2 C).

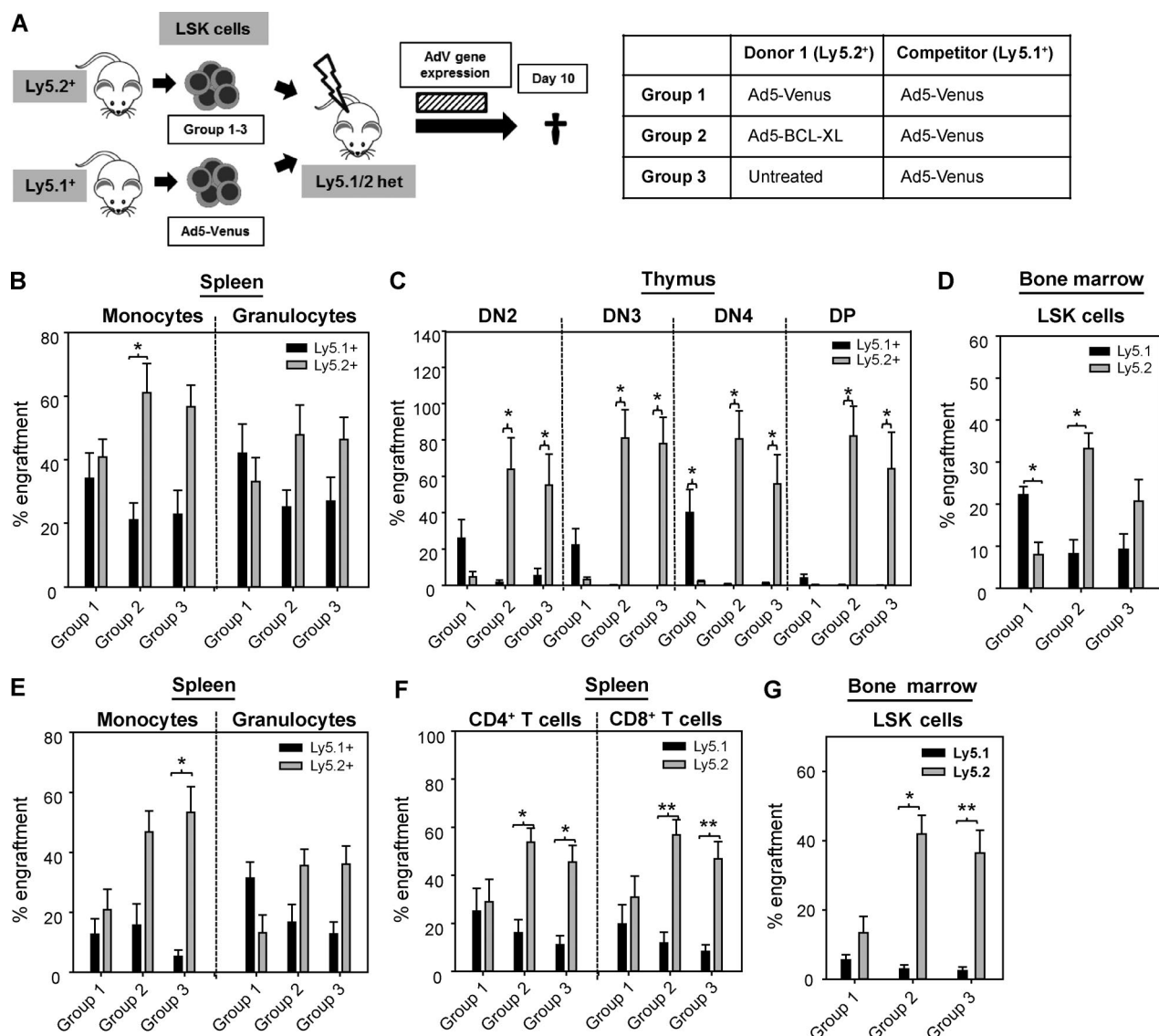## Transient adenoviral BCL-XL overexpression has no leukemogenic potential in vivo

Although we could not find evidence of aberrantly persisting BCL-XL overexpression in the in vitro experiments depicted in Fig. 1, we thoroughly analyzed the presence of BCL-XL–overexpressing hematopoietic clones that could have been generated by constitutive expression caused by random chromosomal integration of adenoviral vectors and persist in vivo (Stephen et al., 2010). Such cells would have had the chance to displace other cells over time (Labi et al., 2013). BM cells isolated from group 2 recipient mice 16 wk after transplantation showed no increase in BCL-XL expression (Fig. 3 A), and splenocytes showed no increased apoptotic resistance to etoposide treatment when compared with cells from group 1 and 3 animals (Fig. 3 B). Importantly, we observed no signs of lympho- or myeloproliferation in six recipient mice transplanted with Ad5–BCL-XL–transduced LSK cells that were monitored for 1 yr (Fig. 3, C and D). Cells isolated from these mice were further used for serial transplantation. Donor cells showed good engraftment, and no detectable signs of lympho- or myeloproliferation were found in secondary recipients (n = 9/group) within 16 wk after transplantation (not depicted).

Stable overexpression of BCL-XL or BCL-2 is not sufficient in itself to transform hematopoietic cells (Strasser et al., 1990). In contrast, overexpression of either protein or deletion of their antagonist BIM strongly accelerates lymphomagenesis in Eµ-MYC transgenic mice (Strasser et al., 1990; Egle et al., 2004). To test the oncogenic potential of transient apoptosis resistance in such a "worst case scenario," we reconstituted lethally irradiated recipients with Eµ-MYC transgenic LSK cells transduced with either Ad5-Venus or Ad5–BCL-XL or left untreated (Fig. 3 E). Recipient mice of all experimental groups developed lymphoma within the same time period (Fig. 3 F). In sum, these data indicate that transient BCL-XL expression in HSPCs does not lead to the accumulation of aberrant cells or accelerate lymphomagenesis on a predisposed genetic background, further documenting the safety of our approach.

Transient pan–caspase inhibition does not sufficiently protect mouse HSPCs from apoptosis in vivo

As adenoviral transduction appears of limited use for therapeutic HSPC manipulation because of toxic effects, we moved on to test whether the pan-caspase inhibitor Q-VD-OPh could serve as an alternative means to block transplantation-associated apoptosis. When LSK cells were continuously treated with Q-VD-OPh in vitro, they were strongly protected from cytokine deprivation–induced apoptosis. Additional inhibition of necroptosis, an alternative type of cell death induced by certain members of the TNF family (e.g., upon viral infection), by Necrostatin-1 (Nec1) further increased cell viability (Fig. S3

Figure 2. **Adenoviral BCL-XL overexpression confers a stable competitive advantage during reconstitution in vivo.** (A) Lethally irradiated heterozygous Ly5.1/Ly5.2 recipient mice were competitively transplanted with Ly5.1$^+$ and Ly5.2$^+$ LSK cells in a 50:50 ratio, which were pretreated as indicated in the table. (B–D) 10 d after transplantation, mice were sacrificed and analyzed. The dashed bar indicates the period of adenoviral gene expression. The Ly5.1$^+$/Ly5.2$^+$ chimerism was determined by flow cytometry in splenic monocytes and granulocytes (B), double-negative (DN) and double-positive (DP) thymocytes (C), and BM-derived LSK cells (D). (E–G) Another set of mice was analyzed 16 wk after transplantation. The Ly5.1$^+$/ Ly5.2$^+$ chimerism was determined by flow cytometry in splenic monocytes and granulocytes (E), T lymphocytes (F), and BM-derived LSK cells (G). Bars represent means of $n = 6$–8 animals of two independent experiments ± SEM. Significant p-values (Wilcoxon test; Ly5.1$^+$ vs. Ly5.2$^+$): (B) Group 2: $P = 0.05$ in monocytes; (C) Group 1: $P = 0.02$ for DN4; Group 2: DN4 and DP, $P = 0.03$ for DN2 and DN3; Group 3: $P = 0.05$ for DN2, $P = 0.03$ for DN3, DN4, and DP; (D) Group 1: $P = 0.03$; Group 2: $P = 0.05$; (E) Group 3: $P = 0.01$ for monocytes; (F) Group 2+3: $P = 0.02$ for CD4$^+$ T cells; $P = 0.01$ for CD8$^+$ T cells; (G) Group 2: $P = 0.02$; group 3: $P = 0.01$.

A). This suggests that a fraction of the cell–autonomous death in vitro may be triggered by autocrine death receptor signaling, but its overall contribution to HSPC cell death appears minor. To test whether HSCT could benefit from transient ex vivo treatment with caspase and necroptosis inhibitors, LSK cells were initially treated with Q-VD-OPh for 24 h, followed by a period of 8 d where the cells were subjected to cytokine deprivation–induced stress in vitro. As shown in Fig. S3 B,

no sustained protective effect could be observed under these conditions. Accordingly, cotransplantation of Ly5.2$^+$ LSK cells treated with Q-VD-OPh (+/− Nec1) and untreated Ly5.1$^+$ LSK cells into Ly5.1/Ly5.2 heterozygous recipients resulted in a similar engraftment with ∼50% Ly5.2$^+$ and 50% Ly5.1$^+$ progeny cells (Fig. S3, C–F). Thus, transient cell death inhibition of isolated LSK cells using a caspase and/or necroptosis inhibitor is not sufficient to promote improved engraftment.

Table 1. **Cellular composition and chimerism of recipient mice transplanted in a competitive manner and analyzed 16 wk later**

Parameter	Group 1 Ly5.1$^+$: Ad5–Venus; Ly5.2$^+$: Ad5–Venus	P–value	Group 2 Ly5.1$^+$: Ad5–Venus; Ly5.2$^+$: Ad5–BCL–XL	P–value	Group 3 Ly5.1$^+$: Ad5–Venus; Ly5.2$^+$: untreated	P–value
BM						
Cells ($\times 10^7$)	5.83 ± 0.46		6.91 ± 0.31		8.08 ± 0.61	
Monocytes ($\times 10^6$)	13.20 ± 1.13		15.32 ± 1.49		16.86 ± 1.30	
Granulocytes ($\times 10^6$)	13.68 ± 2.56		16.55 ± 2.78		17.56 ± 2.92	
B220$^+$IgM$^-$ B cells ($\times 10^6$)	8.49 ± 1.08		9.56 ± 1.17		14.75 ± 1.72	
IgM$^+$ B cells ($\times 10^6$)	5.32 ± 2.98		4.90 ± 2.55		6.97 ± 3.31	
CD4$^+$ T cells ($\times 10^6$)	1.42 ± 0.19		1.60 ± 0.14		1.93 ± 0.21	
CD8$^+$ T cells ($\times 10^6$)	1.19 ± 0.15		1.40 ± 0.12		1.47 ± 0.23	
Ly5.1$^+$ monocytes (%)	20.08 ± 8.2	0.87	20.01 ± 8.1	0.07	9.97 ± 4.0	0.02
Ly5.2$^+$ monocytes (%)	20.85 ± 9.6		52.95 ± 7.4		57.55 ± 9.5	
Ly5.1$^+$ granulocytes (%)	45.08 ± 6.9	0.06	24.51 ± 5.5	0.58	17.50 ± 4.6	0.09
Ly5.2$^+$ granulocytes (%)	11.86 ± 6.4		34.30 ± 7.0		34.86 ± 6.8	
Ly5.1$^+$ B220$^+$IgM$^-$ cells (%)	27.30 ± 9.2	0.87	18.65 ± 6.7	0.04	15.98 ± 5.5	0.04
Ly5.2$^+$ B220$^+$IgM$^-$ cells (%)	23.01 ± 7.6		50,51 ± 6.4		48.36 ± 6.1	
Ly5.1$^+$ B220$^+$IgM$^+$ cells (%)	26.27 ± 10.1	0.87	15.61 ± 7.1	0.04	14.04 ± 5.1	0.03
Ly5.2$^+$ B220$^+$IgM$^+$ cells (%)	21.00 ± 7.3		40.64 ± 5.5		46.68 ± 5.4	
Ly5.1$^+$ CD4$^+$ cells (%)	11.92 ± 3.9	0.40	10.64 ± 3.5	0.02	8.87 ± 3.2	0.03
Ly5.2$^+$ CD4$^+$ cells (%)	19.05 ± 5.3		40.98 ± 5.5		36.25 ± 5.8	
Ly5.1$^+$ CD8$^+$ cells (%)	13.94 ± 5.1	0.24	8.68 ± 2.7	0.01	5.45 ± 2.0	0.01
Ly5.2$^+$ CD8$^+$ cells (%)	28.15 ± 7.5		55.16 ± 7.5		39.33 ± 8.1	
Spleen						
Cells ($\times 10^7$)	6.13 ± 1.30		7.91 ± 1.12		8.22 ± 1.50	
Monocytes ($\times 10^6$)	3.08 ± 0.49		3.55 ± 0.55		3.65 ± 0.31	
Granulocyte ($\times 10^6$)	1.42 ± 0.33		1.49 ± 0.30		1.47 ± 0.35	
B220$^+$IgM$^-$ B cells ($\times 10^6$)	16.8 ± 5.5		23.2 ± 5.1		23.8 ± 5.6	
IgM$^+$ B cells ($\times 10^6$)	17.6 ± 1.11		20.6 ± 1.03		26.2 ± 1.51	
CD4$^+$ T cells ($\times 10^6$)	12.3 ± 2.3		15.4 ± 2.7		16.5 ± 3.1	
CD8$^+$ T cells ($\times 10^6$)	5.70 ± 1.18		7.04 ± 1.43		6.52 ± 1.25	
Thymus						
Cells ($\times 10^7$)	3.76 ± 0.99		4.43 ± 0.54		4.44 ± 0.83	
DN cells ($\times 10^6$)	1.10 ± 0.29		1.72 ± 0.14		1.64 ± 0.38	
DP cells ($\times 10^6$)	27.4 ± 8.6		29.4 ± 5.8		30.2 ± 7.4	
CD4$^+$ SP cells ($\times 10^6$)	4.62 ± 1.10		6.10 ± 0.95		5.69 ± 1.12	
CD8$^+$ SP cells ($\times 10^6$)	0.99 ± 0.24		1.52 ± 0.20		1.56 ± 0.36	
Ly5.1$^+$ DN cells (%)	28.72 ± 10.4	0.50	15.19 ± 7.1	0.02	14.57 ± 5.7	0.03
Ly5.2$^+$ DN cells (%)	36.04 ± 8.7		47.41 ± 6.8		53.70 ± 7.0	
Ly5.1$^+$ DP cells (%)	41.55 ± 14.6	0.74	17.37 ± 9.2	0.05	14.82 ± 7.0	0.07
Ly5.2$^+$ DP cells (%)	29.23 ± 10.7		58.46 ± 8.4		57.40 ± 11.3	
Ly5.1$^+$ CD4$^+$ SP cells (%)	39.55 ± 13.1	0.87	17.19 ± 7.9	0.04	19.40 ± 7.7	0.07
Ly5.2$^+$ CD4$^+$ SP cells (%)	35.62 ± 11.2		58.01 ± 7.4		54.84 ± 10.9	
Ly5.1$^+$ CD8$^+$ SP cells (%)	25.08 ± 11.0	0.24	9.70 ± 4.5	0.01	8.66 ± 3.2	0.01
Ly5.2$^+$ CD8$^+$ SP cells (%)	47.69 ± 12.8		71.70 ± 7.3		65.93 ± 9.9	
Blood						
Cells (/µl)	5,593 ± 10.21		6,436 ± 10.81		6,584 ± 9.64	
Monocytes (/µl)	379 ± 71		610 ± 153		361 ± 42	
Granulocytes (/µl)	702 ± 104		1,240 ± 358		527 ± 96	
B220$^+$IgM$^-$ B cells (/µl)	1,175 ± 363		2,154 ± 333		1,817 ± 279	
IgM$^+$ B cells (/µl)	60 ± 38		44 ± 17		62 ± 28	
CD4$^+$ T cells (/µl)	891 ± 142		1,089 ± 144		865 ± 91	
CD8$^+$ T cells (/µl)	526 ± 104		641 ± 92		475 ± 60	
Ly5.1$^+$ monocytes (%)	23.43 ± 8.8	0.87	26.47 ± 11.8	0.26	10.27 ± 4.1	0.01
Ly5.2$^+$ monocytes (%)	21.20 ± 8.0		50.56 ± 8.0		60.36 ± 9.9	
Ly5.1$^+$ granulocytes (%)	56.70 ± 8.9	0.04	32.54 ± 8.9	0.58	25.50 ± 7.0	0.26
Ly5.2$^+$ granulocytes (%)	15.25 ± 6.5		38.59 ± 6.6		42.54 ± 7.6	
Ly5.1$^+$ B220$^+$IgM$^-$ cells (%)	25.28 ± 9.7	0.61	20.64 ± 6.8	0.03	16.42 ± 6.8	0.03
Ly5.2$^+$ B220$^+$IgM$^-$ cells (%)	36.30 ± 11.3		57.08 ± 7.0		62.93 ± 8.0	
Ly5.1$^+$ B220$^+$IgM$^+$ cells (%)	38.38 ± 13.1	0.47	25.37 ± 8.5	0.22	23.39 ± 8.9	0.08
Ly5.2$^+$ B220$^+$IgM$^+$ cells (%)	27.41 ± 13.7		53.97 ± 10.9		52.57 ± 10.3	
Ly5.1$^+$ CD4$^+$ cells (%)	28.06 ± 12.1	0.61	19.32 ± 6.8	0.07	17.67 ± 4.9	0.04

Parameter	Group 1		Group 2		Group 3	
	Ly5.1$^+$: Ad5–Venus; Ly5.2$^+$: Ad5–Venus	P-value	Ly5.1$^+$: Ad5–Venus; Ly5.2$^+$: Ad5–BCL-XL	P-value	Ly5.1$^+$: Ad5–Venus; Ly5.2$^+$: untreated	P-value
Ly5.2$^+$ CD4$^+$ cells (%)	30.01 ± 11.4		49.75 ± 6.4		49.37 ± 7.2	
Ly5.1$^+$ CD8$^+$ cells (%)	19.60 ± 8.3	0.40	13.16 ± 4.5	0.02	9.95 ± 3.2	0.01
Ly5.2$^+$ CD8$^+$ cells (%)	31.08 ± 8.8		52.66 ± 7.0		46.37 ± 7.3	

The transplantation procedure and groups are defined in Fig. 3. Values represent means of *n* = 7–8 animals from three independent experiments ± SEM. Significant p-values with regard to the Ly5.1$^+$/Ly5.2$^+$ ratio are indicated (Wilcoxon test). DN, double negative; DP, double positive; SP, single positive.

Transient transduction of full–length BCL–XL protein protects LSK cells from apoptosis in vitro

We next explored a system of nonviral delivery of BCL–XL into LSK cells. Protein transduction represents a safe alternative to viral gene transfer without the risk of genomic integration or recombination events. Cellular protein uptake is enabled by cell-penetrating peptides (CPPs) mainly composed of positively charged amino acids (Reissmann, 2014). The protein transduction domain (PTD) from the HIV TAT protein (TAT$_{48-57}$) was chosen as the CPP. In our first approach, we used a commercially available fusion of the TAT-PTD to the BCL-2 homology domain 4 (BH4) domain of human BCL–XL (HIV-TAT$_{48-57}$-β-Ala–BCL-XL BH$_{44-23}$, sequence: Ac-GRKKRRQRRR-βA-SNRELVVDFLSY KLSQKGYS-OH). The BH4 domain was shown to be relevant for the antiapoptotic function of BCL-2 and BCL-XL and to inhibit apoptosis even as an isolated domain (Huang et al., 1998; Sugioka et al., 2003). In various in vitro and in vivo mouse models, TAT-BH4 treatment resulted in protection from apoptosis (Klein et al., 2004; Hotchkiss et al., 2006; Donnini et al., 2009). However, despite its efficient cellular uptake and mitochondrial localization, TAT-BH4 did not confer any protection to LSK cells subjected to the cytotoxic agents Taxol and etoposide (Fig. S4, A–C).

Next, we bacterially expressed full–length mouse Bcl-xL protein coupled to the TAT-PTD (6xHis-TAT$_{49-57}$(RKK RRQRRR)–Bcl-xL–HA) and purified it to homogeneity using metal affinity chromatography. LSK cells were incubated with 1.5 µM TAT–Bcl-xL for 2 h, and protein uptake was measured after 24 h by intracellular flow cytometry and fluorescence microscopy using an anti–Bcl-xL antibody. We observed pronounced cellular uptake (Fig. 4 A) and mitochondrial as well as cytoplasmic localization of the protein (Fig. 4 B). To verify correct localization by a different method, we transduced HeLa cells with TAT–Bcl-xL and harvested cells at different time points. Fractionated Western blotting analysis was performed 24 h after transduction and confirmed the localization of TAT–Bcl-xL to the cytosol and mitochondria (Fig. S5 A), mimicking the localization of the endogenous protein (Edlich et al., 2011). Time kinetics revealed a rapid decrease of TAT–Bcl-xL protein within the first 24 h upon uptake with the appearance of a shorter fragment, indicating protein degradation (Fig. S5 B). Occurrence of the short protein fragment could not be prevented by proteasome inhi-

bition using MG132, indicating that the protein was, at least in part, degraded in a nonproteasomal manner (Fig. S5 C), most likely in lysosomes. Functional assays showed that TAT–Bcl-xL protein transduction resulted in a robust protection of LSK cells from apoptosis induced by etoposide or cytokine deprivation for 6–8 d (Fig. 4, C and D). During this time period, TAT–Bcl-xL protein content decreased gradually and more rapidly in proliferating cells (Fig. 4 E). Hence, we show here that recombinant TAT–Bcl-xL transiently and efficiently protects LSK cells from stress-induced apoptosis in vitro.

Protein transduction of full–length Bcl–xL increases LSK cell fitness in vivo

Increased resistance to apoptosis should confer competitive advantages to cells, particularly under conditions of stress. To investigate the effects of TAT–Bcl-xL on HSPC competitiveness, we transduced LSK cells isolated from Ly5.1$^+$ or Ly5.2$^+$ mice with TAT–Bcl-xL and co-cultured these cells with untreated LSK cells in a 50:50 ratio. Even under optimal culture conditions (i.e., media supplemented with 10% serum and the cytokines Flt3L, SCF, and TPO), TAT–Bcl-xL transduction conferred a competitive advantage, indicating that apoptosis took place during expansion (Fig. 5 A). Upon cytokine deprivation or treatment with etoposide, the Ly5.1/Ly5.2 ratio was strongly biased in favor of TAT–Bcl-xL–treated cells, demonstrating a strong protective effect during stress-induced apoptosis (Fig. 5, B and C). Encouraged by this finding, we performed competitive reconstitution experiments in mice using Ly5.2$^+$ cells incubated with TAT–Bcl-xL for 2 h prior transplantation and Ly5.1$^+$ competitor cells left untreated (50:50 ratio; Fig. 5 D). 16 wk after transplantation, the ratio was found shifted strongly in favor of TAT–Bcl-xL–treated Ly5.2$^+$ cells (group 2; Fig. 5, E–G; and Table 2). Altogether, we have shown that recombinant Bcl-xL introduced prior transplantation and transiently expressed for 6–8 d confers substantial fitness to mouse HSPCs, leading to a competitive advantage and a superior transplantation outcome.

Uptake of TAT–BCL-XL by human CD34$^+$ cells results in protection from apoptosis in vitro

We have previously shown that the proapoptotic functions of BIM and BMF during transplantation-associated apoptosis are conserved between mouse and human HSPCs (Labi et al., 2013). Because of our encouraging results with mouse
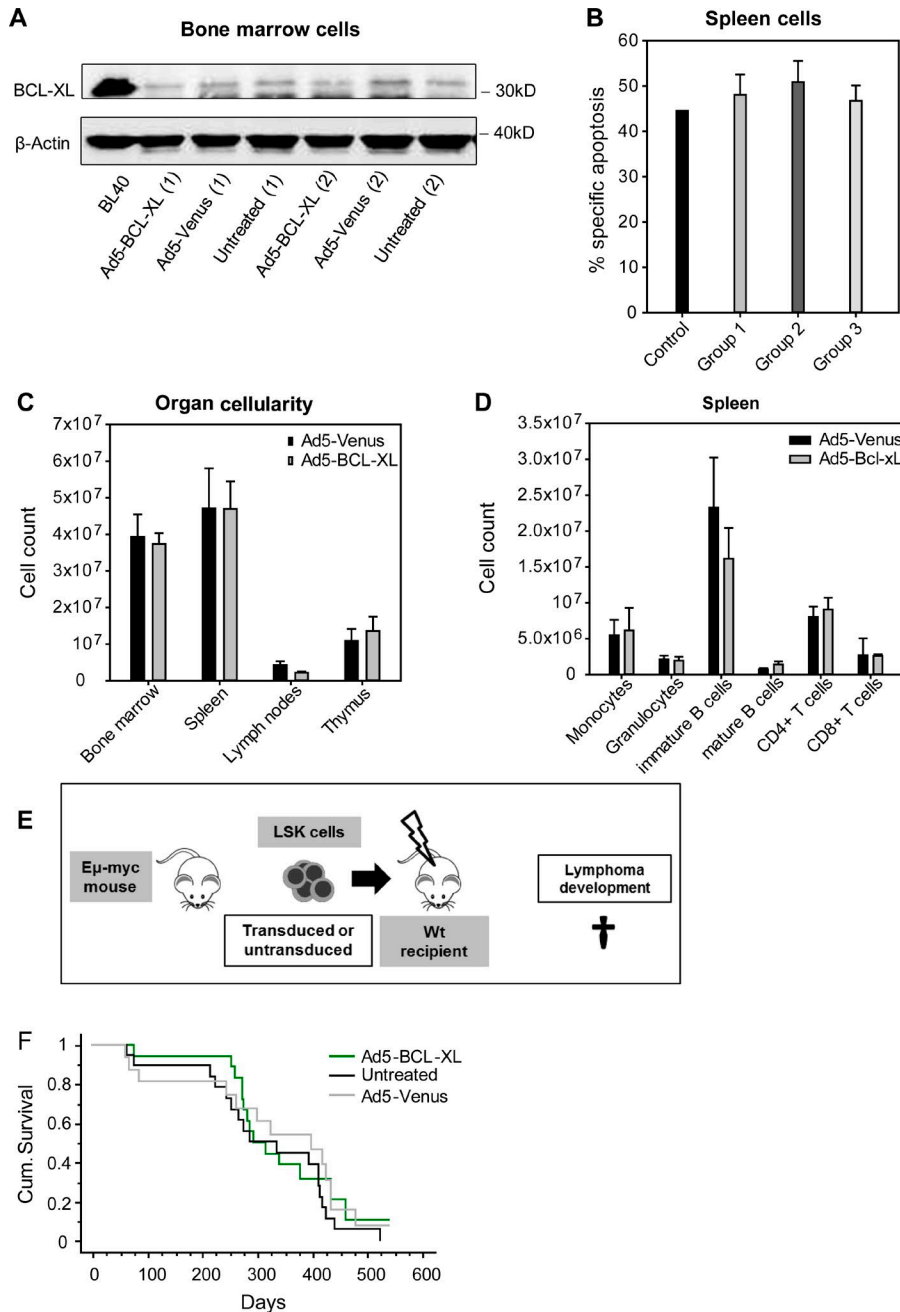
Figure 3. Adenoviral BCL-XL overexpression has no long-term adverse effects. (A) Recipient mice were transplanted as indicated in Fig. 2 A and sacrificed 16 wk later. Total BM cells were analyzed for their BCL-XL protein contents by Western blot. The Burkitt lymphoma cell line BL40 was used as positive control and β-actin as loading control. The legend indicates how the Ly5.2+ donor cells were treated before transplantation. (B) Splenic cells of recipient mice were cultured for 24 h in the presence or absence of etoposide (1 μg/ml), and specific apoptosis was determined by flow cytometry. Spleens of WT mice were used as a control. Bars represent means of $n = 3$ independent experiments ± SEM. No significant differences were observed (Mann–Whitney test). (C and D) Ly5.1+ recipient mice were transplanted with 15,000 Ly5.2+ LSK cells transduced with Ad5-Venus or Ad5–Bcl-xL. To ensure survival of the recipients, 150,000 Ly5.1+ BM cells were co-transplanted. Recipient mice were sacrificed 1 yr later and analyzed in detail. No signs of myelo- or lymphoproliferation or leukemia were observed in the indicated organs. Bars represent means of $n = 6$ animals ± SEM; no significant differences were observed (Mann–Whitney test). (E) LSK cells were isolated from the BM of Eμ-myc tg mice and left untreated or transduced with the Ad5-Venus or Ad5–BCL-XL adenoviruses. Subsequently, LSK cells were transduced into lethally irradiated recipient mice, which were monitored for lymphoma development. (F) When in poor general condition, recipient mice were sacrificed and analyzed. The Kaplan–Meier blot shows $n = 13$–18 mice per group (four independent experiments). No significant p-values between the groups were obtained by using the log-rank (Mantel–Cox) test.

LSK cells, we reached out to extend the protein transduction approach to human cord blood–derived CD34+ cells. To this aim, we generated a human BCL-XL protein coupled to the TAT sequence (TAT–BCL-XL). 2-h incubation of human cord blood–derived CD34+ cells with TAT–BCL-XL resulted in inefficient protein uptake (Fig. 6 A). Efficiency of protein uptake could not be increased by using higher protein concentrations (up to 6 μM), optimized media conditions, longer incubation periods, or repeated addition of recombinant protein to the cells as performed by Krosl et al. (2003) for TAT-HOXB4 (not depicted). Neither replac-

ing dextran sulfate with methyl-β-cyclodextrin, known to deplete cholesterol from the cell surface, nor using a combination thereof at different temperatures (4°C, 30°C, and 37°C) to allow for different ways of protein uptake (membrane diffusion vs. endocytosis) improved uptake efficiency. Moreover, the use of a Chariot reagent to stimulate protein uptake in a TAT-independent way was also unsatisfactory. However, the few CD34+ cells that were successfully transduced with TAT–BCL-XL were efficiently protected from cytokine deprivation–induced apoptosis as reflected by their strong accumulation (Fig. 6 B) and the reduced rate of spe-
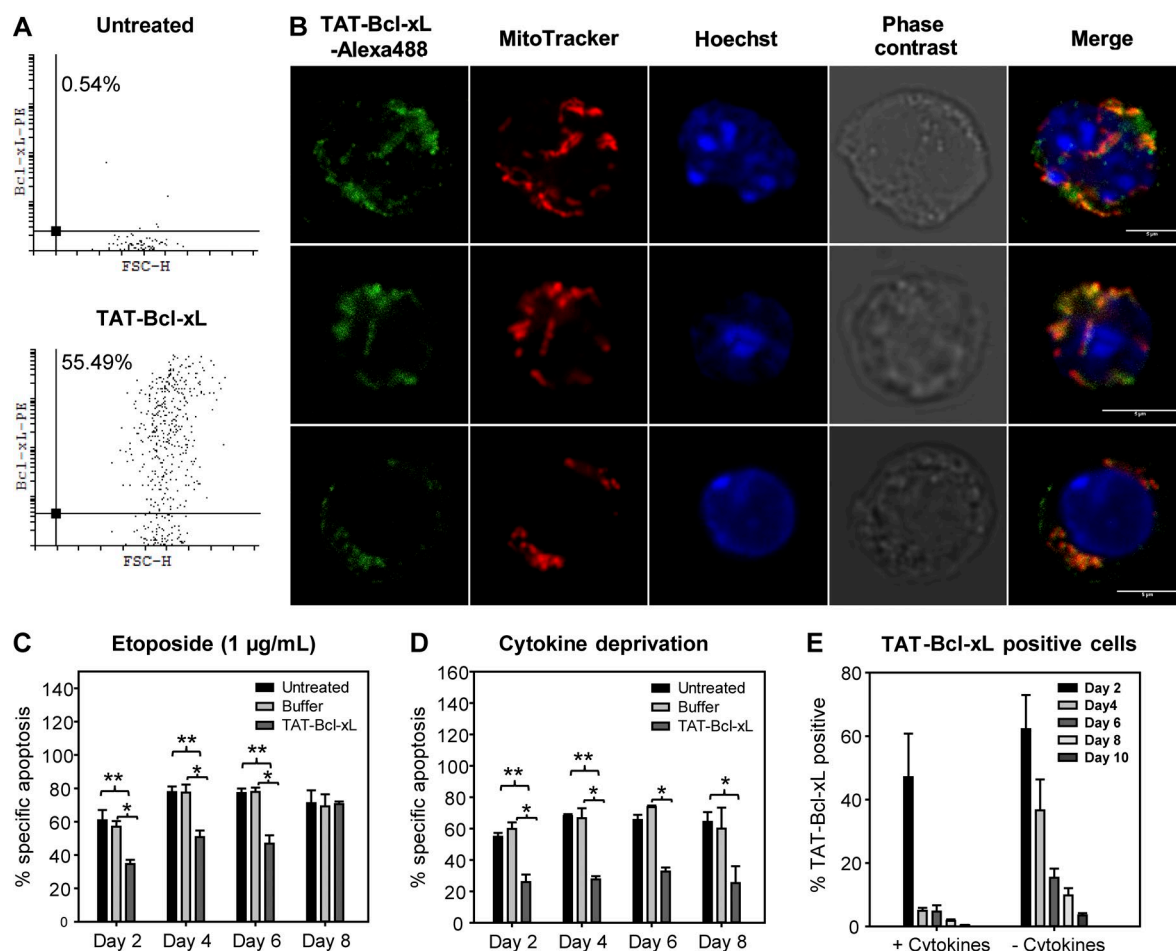
Figure 4. **TAT–Bcl–xL protein is efficiently taken up by LSK cells and inhibits apoptosis.** (A) WT LSK cells were treated with dextran sulfate for 30 min and TAT–Bcl–xL for 2 h (1.5 μM). Protein content was determined 48 h later by flow cytometry using an anti–Bcl–xL antibody. (B) Localization of TAT–Bcl–xL protein in LSK cells was determined 24 h after protein transduction by fluorescence microscopy and shows TAT–Bcl–xL on mitochondria and in the cytoplasm. Bars, 5 μm. (C and D) LSK cells transduced with TAT–Bcl–xL protein were subjected to 1 μg/ml etoposide (C) or cytokine withdrawal (D). Specific apoptosis was determined by flow cytometry at indicated time points. Bars represent means of n = 4 independent experiments ± SEM. Significant p–values (Mann–Whitney test): (C) Untreated vs. TAT–Bcl–xL: P = 0.005 on day 2 and P = 0.01 at day 4 and 6; Buffer vs. TAT–Bcl–xL: P = 0.02 at day 2, 4, and 6; (D) Untreated vs. TAT–Bcl–xL: P = 0.005 at day 2 and 8, P = 0.01 at day 4, P = 0.02 at day 6; Buffer vs. TAT–Bcl–xL: P = 0.02 at day 2, P = 0.03 at day 4 and 6. (E) TAT–Bcl–xL–treated LSK cells were cultured in the presence or absence of cytokines. At the indicated time points, TAT–Bcl–xL–positive cells were determined by intracellular flow cytometry. Bars represent means of n = 4 independent experiments ± SEM.

cific apoptosis over 6 d of culture (Fig. 6 C). In summary, TAT–BCL–XL protein transduction can be used to increase the viability of human CD34^{+} cells subjected to stress stimuli usually occurring during the period of transplantation and early engraftment.

DISCUSSION

Inhibition of the proapoptotic proteins BIM and BMF strongly improved performance of mouse and human HSPCs during transplantation (Labi et al., 2013), but this was associated with an increased risk of malignant transformation and autoimmunity in recipient mice (Labi et al., 2014). Thus, inhibiting apoptosis transiently during the stressful period of transplantation (from HSPC isolation to homing and resumption of hemato-

poiesis) might be an attractive strategy to improve HSCT outcome without increasing the risk of long-term adverse effects.

Apoptosis of HSPCs could be inhibited at different levels. Stimulation with the cytokines SCF and Flt3L increases cell viability at least partially by inhibiting *Bim* and *Bmf* mRNA expression (Labi et al., 2013), but these cytokines promote proliferation and differentiation at the expense of self–renewing LT–HSCs. Inhibition of caspases, the executioners of apoptosis, appears to be a straightforward approach, but our experiments revealed that using a pan–caspase inhibitor before transplantation does not improve transplantation outcome. One shortcoming of caspase inhibition is that it cannot prevent mitochondrial damage and loss of function, which can cause cell death even in the absence of active
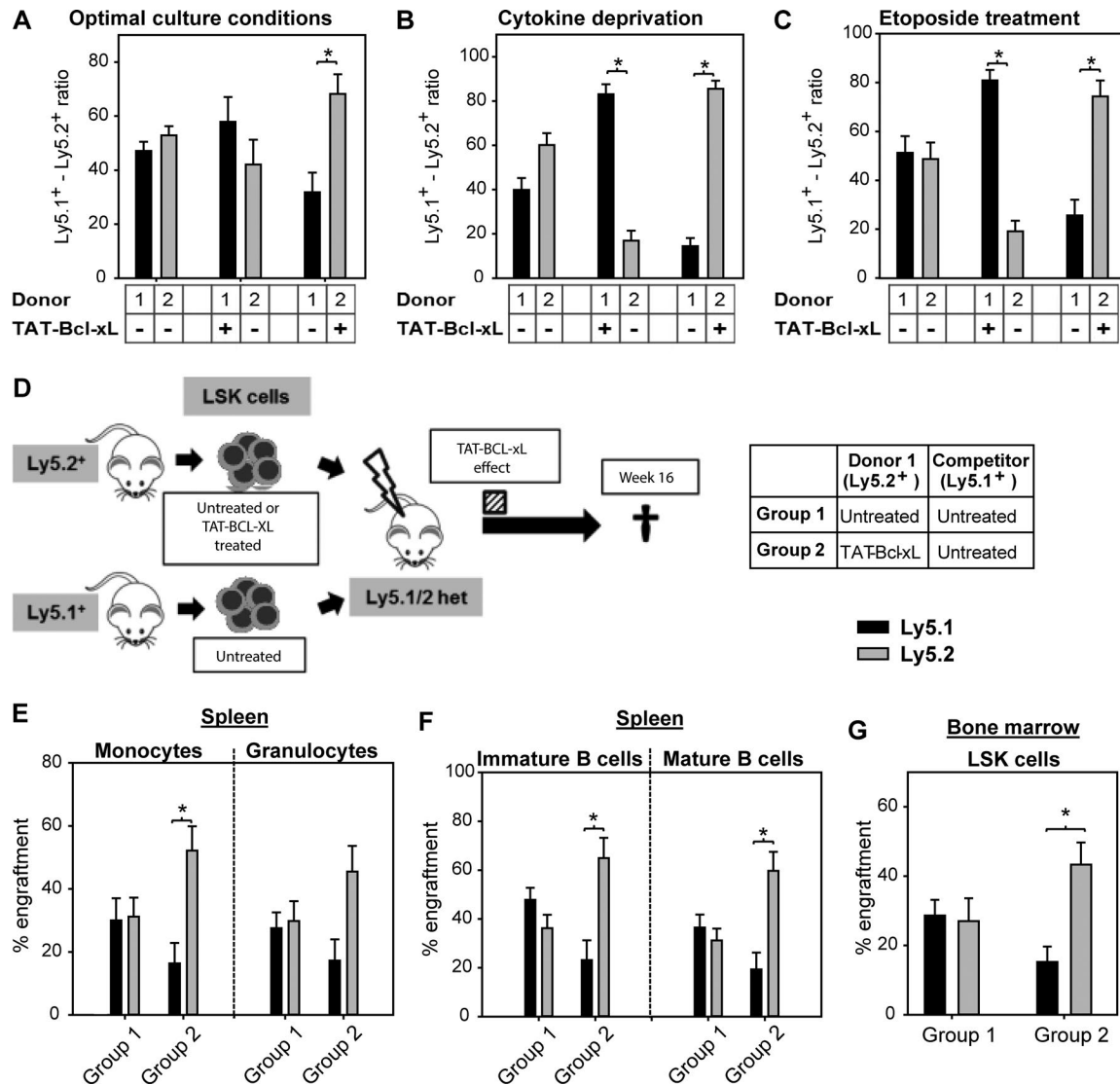
Figure 5. **TAT–Bcl–xL protein transduction increases competitiveness of LSK cells in vitro and in vivo.** (A–C) Ly5.1⁺ and Ly5.2⁺ LSK cells were cultured in a 50:50 ratio under different culture conditions. Cells were either pretreated with TAT–Bcl–xL or left untreated and cultured for 5 d under optimal culture conditions (10% serum with SCF, TPO, and Flt3L, 100 ng/ml each; A), in the absence of cytokines (B), or in the presence of etoposide (C). Bars represent means of $n = 4$ independent experiments $\pm$ SEM. Significant p-values (Wilcoxon Test): P = 0.04 in A–C. (D) Ly5.2⁺ LSK cells treated either with TAT–Bcl–xL or left untreated were co-transplanted with untreated Ly5.1⁺ cells in a 50:50 ratio into lethally irradiated Ly5.1/Ly5.2 heterozygous mice. 16 wk later, recipient mice were sacrificed, and donor chimerism was determined by flow cytometry. The dashed bar indicates the period, in which Ly5.2⁺ LSK cells were containing TAT–Bcl–xL. (E–G) Chimerism was detected in splenic monocytes and B and T lymphocytes (E and F), as well as in BM-derived LSK cells (G). Bars represent means $\pm$ SEM of $n = 10$–11 mice from three independent experiments. Significant p-values (Wilcoxon test): (E) P = 0.02 for Group 2 in monocytes; (F) P = 0.03 for Group 2 in immature and mature B cells; (G) P = 0.03 for Group 2 in LSK cells.

caspases (White et al., 2014). We are thus convinced that the most promising approach to transient apoptosis inhibition in HSPCs is to manipulate the equilibrium between pro- and antiapoptotic Bcl-2 family members, the "integration device" that controls survival–death decisions upstream of mitochondria. Increasing the amount of antiapoptotic BCL-XL is particularly attractive, because it antagonizes BIM and BMF, as well as BAK and BAX, thereby stabilizing mitochondrial integrity. One major advantage of this approach is that a plethora

of different stress signals converge at the level of the BCL-2 family. Higher BCL-XL levels thus can be protective, even if upstream signals and pathways have not been fully characterized. Although it can be anticipated that loss of niche signals are responsible for apoptosis, the specific proteins and signaling pathways involved in transplantation-induced apoptosis have only been partially identified (e.g., cytokine deprivation; Murray et al., 1999; Varnum-Finney et al., 2000; Gerber et al., 2002; Butler et al., 2010).

Table 2. **Cellular composition and chimerism of recipient mice transplanted in a competitive manner and analyzed 16 wk later**

Parameter	Group 1		Group 2	
	Ly5.1$^+$: untreated; Ly5.2$^+$: untreated	P-value	Ly5.1$^+$: untreated; Ly5.2$^+$: TAT–Bcl–xL	P-value
BM				
Cells (×10^7)	3.58 ± 0.48		3.83 ± 3.22	
Monocytes (×10^6)	4.88 ± 1.05		4.64 ± 0.79	
Granulocytes (×10^6)	10.4 ± 1.9		1,000 ± 110	
B220$^+$IgM$^-$ B cells (×10^6)	2.86 ± 0.46		3.81 ± 0.34	
IgM$^+$ B cells (×10^6)	2.21 ± 0.42		2.60 ± 0.34	
CD4$^+$ T cells (×10^6)	0.34 ± 0.05		0.47 ± 0.05	
CD8$^+$ T cells (×10^6)	0.62 ± 0.09		0.71 ± 0.10	
Ly5.1$^+$ monocytes (%)	29.64 ± 7.65	0.28	20.93 ± 8.50	0.03
Ly5.2$^+$ monocytes (%)	44.25 ± 8.85		63.32 ± 10.70	
Ly5.1$^+$ granulocytes (%)	33.32 ± 6.20	0.65	21.24 ± 7.35	0.05
Ly5.2$^+$ granulocytes (%)	40.24 ± 8.13		59.29 ± 11.03	
Ly5.1$^+$ B220$^+$IgM$^-$ cells (%)	36.26 ± 6.41	0.80	14.37 ± 6.78	0.02
Ly5.2$^+$ B220$^+$IgM$^-$ cells (%)	35.87 ± 7.59		63.61 ± 8.45	
Ly5.1$^+$ B220$^+$IgM$^+$ cells (%)	44.41 ± 5.10	0.58	17.40 ± 7.41	0.04
Ly5.2$^+$ B220$^+$IgM$^+$ cells (%)	33.87 ± 5.89		64.61 ± 7.72	
Ly5.1$^+$ CD4$^+$ cells (%)	22.79 ± 2.95	0.72	10.81 ± 2.75	0.006
Ly5.2$^+$ CD4$^+$ cells (%)	21.77 ± 3.64		38.55 ± 3.83	
Ly5.1$^+$ CD8$^+$ cells (%)	31.45 ± 2.43	0.01	16.40 ± 4.34	0.11
Ly5.2$^+$ CD8$^+$ cells (%)	16.21 ± 2.17		31.01 ± 3.98	
Spleen				
Cells (×10^7)	11.70 ± 0.86		12.29 ± 0.73	
Monocytes (×10^6)	4.36 ± 0.85		2.88 ± 0.38	
Granulocytes (×10^6)	2.68±0.43		1.76±0.25	
B220$^+$IgM$^-$ B cells (×10^6)	30.5±9.3		35.2±7.1	
IgM$^+$ B cells (×10^6)	37.7 ± 6.1		39.2±6.4	
CD4$^+$ T cells (×10^6)	19.7 ± 2.0		19.3±1.6	
CD8$^+$ T cells (×10^6)	9.89 ± 0.69		9.27±0.62	
Thymus				
Cells (×10^7)	6.86 ± 0.84		4.64 ± 0.86	
DN cells (×10^6)	1.86 ± 0.51		2.12 ± 0.63	
DP cells (×10^6)	49.3 ± 6.4		31.0 ± 6.9	
CD4$^+$ SP cells (×10^6)	5.66 ± 1.09		4.68 ± 0.95	
CD8$^+$ SP cells (×10^6)	3.46 ± 1.26		2.37 ± 0.49	
Ly5.1$^+$ DN cells (%)	48.93 ± 6.77	0.11	21.54 ± 6.39	0.05
Ly5.2$^+$ DN cells (%)	27.26 ± 7.37		55.24 ± 8.51	
Ly5.1$^+$ DP cells (%)	60.36 ± 12.24	0.14	25.28 ± 10.85	0.08
Ly5.2$^+$ DP cells (%)	24.80 ± 10.56		63.75 ± 11.49	
Ly5.1$^+$ CD4$^+$ SP cells (%)	65.47 ± 9.92	0.08	26.22 ± 10.13	0.08
Ly5.2$^+$ CD4$^+$ SP cells (%)	27.34 ± 9.31		64.46 ± 10.33	
Ly5.1$^+$ CD8$^+$ SP cells (%)	54.04 ± 10.81	0.33	17.74 ± 8.23	0.02
Ly5.2$^+$ CD8$^+$ SP cells (%)	36.31 ± 9.87		70.23 ± 10.26	
Blood				
Cells (/µl)	10,755 ± 895		10,391 ± 799	
Monocytes (/µl)	616 ± 78		422 ± 62	
Granulocytes (/µl)	970 ± 111		685 ± 99	
B220$^+$IgM$^-$ B cells (/µl)	3,821 ± 822		3,562 ± 560	
IgM$^+$ B cells (/µl)	1,845 ± 437		2,188 ± 502	
CD4$^+$ T cells (/µl)	1,803 ± 178		1,746 ± 135	
CD8$^+$ T cells (/µl)	1,073 ± 103		1,006 ± 77	
Ly5.1$^+$ monocytes (%)	46.34 ± 8.69	0.65	27.44 ± 9.23	0.11
Ly5.2$^+$ monocytes (%)	38.05 ± 8.96		60.49 ± 9.36	
Ly5.1$^+$ granulocytes (%)	45.74 ± 6.60	0.39	29.14 ± 8.58	0.18
Ly5.2$^+$ granulocytes (%)	38.28 ± 7.59		56.30 ± 9.90	
Ly5.1$^+$ B220$^+$IgM$^-$ cells (%)	45.24 ± 5.19	0.88	21.64 ± 8.10	0.03
Ly5.2$^+$ B220$^+$IgM$^-$ cells (%)	38.42 ± 6.10		66.00 ± 8.74	
Ly5.1$^+$ B220$^+$IgM$^+$ cells (%)	38.33 ± 4.94	0.96	18.24 ± 7.46	0.02
Ly5.2$^+$ B220$^+$IgM$^+$ cells (%)	34.51 ± 5.38		60.74 ± 8.12	
Ly5.1$^+$ CD4$^+$ cells (%)	56.86 ± 4.88	0.02	29.47 ± 8.29	0.18
Ly5.2$^+$ CD4$^+$ cells (%)	23.67 ± 4.84		49.59 ± 8.13	

Table 2.   **Cellular composition and chimerism of recipient mice transplanted in a competitive manner and analyzed 16 wk later** *(Continued)*

Parameter	Group 1			Group 2	
	Ly5.1⁺: untreated; Ly5.2⁺: untreated	P-value		Ly5.1⁺: untreated; Ly5.2⁺: TAT–Bcl-xL	P-value
Ly5.1$^+$ CD8$^+$ cells (%)	45.71 ± 3.43	0.01		23.69 ± 5.43	0.11
Ly5.2$^+$ CD8$^+$ cells (%)	19.22 ± 3.14			37.96 ± 5.71	

The transplantation procedure and groups are defined in Fig. 5 D. Values represent means of *n* = 10–11 animals of three independent experiments ± SEM. Significant p-values with regard to the Ly5.1⁺/Ly5.2⁺ ratio are indicated (Wilcoxon test). DN, double negative; DP, double positive; SP, single positive.

Here, we achieved transient apoptosis inhibition through BCL-XL overexpression by either adenoviral vectors or ex vivo transduction of recombinant protein. Both methods resulted in the protection of mouse LSK cells from cytokine-induced apoptosis in vitro (6–8 d) and conferred promising in vivo advantages in transplantation experiments, which were detected as soon as 10 d after transplantation and remained stable over time. 16 wk after transplantation, most hematological cells were still derived from those LSK cells that intermittently had overexpressed BCL-XL, indicating a successful manipulation of LT-HSCs, the cells that are required for lifelong hematopoiesis. Whereas the method of adenoviral infection itself resulted in toxicity and thus poor engraftment of mouse LSK cells, the protein transduction approach appeared superior. Although full-length BCL-XL showed strong antiapoptotic activity, its isolated BH4 domain did not inhibit LSK cell apoptosis. This observation contrasts those of earlier studies (Sugioka et al., 2003; Klein et al., 2004; Hotchkiss et al., 2006; Donnini et al., 2009) but is corroborated by recent work showing that the BH4 domain is primarily involved in Ca^{2+} signaling (Monaco et al., 2015).

A key question concerning clinical applicability is whether transient apoptosis inhibition in donor cells is harmful to the recipient by paving the way for leukemia. Conceptually, short-term apoptosis resistance should keep HSPCs alive during the time of inadequate supply with prosurvival signals but not suffice to promote transformation. Seriously damaged donor cells or cells carrying aberrantly activated oncogenic signaling should undergo apoptosis upon sufficient decline of exogenous BCL-XL levels. Along this line, short-term resistance to apoptosis did not cause or accelerate malignant transformation on either a WT or premalignant background. One potential threat could emerge from possible rare integration or recombination events of adenoviruses. Although we could not detect evidence of viral integration or permanent BCL-XL overexpression, such a risk cannot be entirely ruled out. In contrast, protein transduction of BCL-XL does not involve genetic material and is thus not associated with a similar risk.

To analyze the immediate translational potential of our work, we applied the protein transduction protocol to human cord blood–derived CD34$^+$ cells. Although protein uptake by CD34$^+$ cells was rather poor, TAT–BCL-XL robustly protected CD34$^+$ cells from cytokine deprivation–induced apoptosis for up to 6 d. In the longer term, the exchange of the CPP or the use of "sneaking ligands" specific for human CD34 could be envisioned to optimize protein transduction (Shen et al., 2004; Sehnert et al., 2015). Nevertheless, direct inhibition of BIM and BMF or BAX and BAK by small-molecule drugs might be a superior strategy. As specific BAX/BAK inhibitors are currently under development, the need for efficient protein uptake in human HSPCs might soon be dispensable.

In sum, we show that transient apoptosis inhibition for 6–8 d during the engraftment period is sufficient to positively influence hematopoietic engraftment of donor HSPCs without increasing the risk of malignant transformation. Considering the relevance of HSCT for many hematological, immunological, and malignant diseases, our contribution is of high value, especially for patients who do not yet have access to HSCT because of the lack of a suitable donor (Mogul, 2000). In particular, our approach could secure increased access of adult patients to UCB transplantation and improve graft quality in case of long transport routes or when cell separation is required before infusion (e.g., blood group incompatibility). Other possible fields of application would be HSCT after reduced-intensity conditioning or haploidentical transplantation, two situations in which donor stem cells are strongly challenged and require special fitness to survive the hostile environment (Handgretinger et al., 2001; Ball et al., 2005). Generally, our approach will be beneficial for all patients undergoing HSCT. Transplantation of particularly fit and stress-resistant donor HSPCs will minimize the risk of graft failure and accelerate hematopoietic regeneration, thus reducing transplantation-associated morbidity and mortality caused by infections and bleeding.

Our approach to transient apoptosis inhibition has the potential to be used for other forms of cell therapy. Granulocyte transfusions are strongly restricted by the very short half-life of granulocytes (7–8 h). It has been shown that overexpression of antiapoptotic BCL-2 protein results in prolonged granulocyte survival (Villunger et al., 2003). Similarly, transfused platelets have a half-life of hours to days and undergo apoptosis in a BAK-dependent manner that is inhibited by BCL-XL. The required transfusion frequency for granulocytes or platelets might therefore be strongly reduced by BCL-XL transduction or BAX/BAK inhibition. In all of these settings, donor cells can be manipulated ex vivo, and no additional in vivo treatment of the donor and/or recipient is required, thus preventing systemic side effects. Over the long run, our approach to transient apoptosis inhibition could also be used to prevent myelosuppression during chemotherapy against solid cancers. In such a scenario, antiapoptotic substances must be
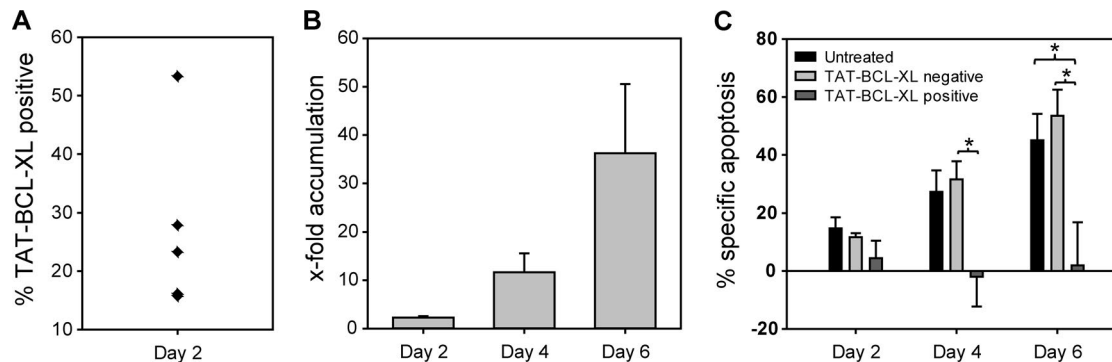
Figure 6. Human TAT–BCL-XL protein protects human CD34^{+} cells under conditions of stress. (A) Fresh cord blood derived CD34^{+} cells were treated with dextran sulfate (100 µg/ml) for 30 min and TAT–BCL-XL (1.5 µM) for 2 h in serum-free medium. At day 2, TAT–BCL-XL–positive cells were determined by intracellular flow cytometry using an anti–BCL-XL antibody. (B) TAT–BCL-XL–treated or untreated CD34^{+} cells were cultured in the presence or absence of rhSCF, rhFlt3L (100 ng/ml each), rhTPO (50 ng/ml), and rhIL3 (20 ng/ml) for 6 d. At days 2, 4, and 6, percentage of TAT–BCL-XL–positive cells was determined by flow cytometry. Bars represent x-fold accumulation = (%TAT–BCL-XL[+] in absence of cytokines)/(%TAT–BCL-XL[+] cultured with cytokines). (C) At days 2, 4, and 6, apoptosis was determined in the different cell populations (untreated, TAT–BCL-XL–negative, and TAT–BCL-XL–positive cells) by flow cytometry, and the percent specific apoptosis was determined. Bars represent means of $n = 5$ from four independent experiments $\pm$ SEM. Significant p-values (Mann-Whitney test): (C) $P = 0.02$ for TAT–BCL-XL negative vs. TAT–BCL-XL positive on day 4; $P = 0.04$ for untreated vs. TAT–BCL-XL positive and TAT–BCL-XL negative vs. TAT–BCL-XL positive.

delivered strictly and exclusively to BM CD34^{+} cells, and their uptake by cancer cells must be prevented by all means. It can be expected that novel achievements of targeted drug delivery will eventually enable such an application.

MATERIALS AND METHODS

Mice

C57BL/6 WT (Ly5.2), B6.SJL-*Ptprc*ᵃ*Pepc*ᵇ/BoyJ (Ly5.1), Ly5.1/Ly5.2 heterozygous, and C57BL/6-*Rag1*^{−/−} mice (Mombaerts et al., 1992) were used for transplantation experiments. In addition, B6.Cg-Tg(IghMyc)22Bri/J (Eµ-*MYC* tg) mice were used (Harris et al., 1988). All recipient mice were kept under specific pathogen–free conditions and received enrofloxacin for transplantation (−1 wk to +4 wk). All experiments were performed according to the guidelines of German laws regarding animal experiments and approved by local committees (RP Freiburg/Germany).

Cell isolation and culture

Mouse LSK cells were isolated by magnetic bead depletion of lineage marker–positive cells (MACS lineage cell depletion kit containing antibodies for CD5, B220, CD11b, Gr-1, 7–4, and Ter-119; Miltenyi) and subsequent sorting of viable (7-AAD–negative) sca-1[+]c-kit^{+} cells using a MoFlo Astrios sorter (Beckman Coulter). LSK cells were cultured in IMDM (PAA) supplemented with 0.5 mg/ml penicillin and 0.5 mg/ml streptomycin (Sigma), 10% FCS (PAA), and the recombinant mouse cytokines SCF, TPO, and Flt3L (100 ng/ml each; Immunotools). Where indicated, cells were cultured in the absence of cytokines or treated with 1 µg/ml etoposide (Sigma-Aldrich), 30 µg/ml Taxol (Sigma-Aldrich), 50 µM Q-VD-OPh (MP Biomedicals), and/or 50 µM Nec1 (Merck).

Human UCB was obtained immediately after caesarean birth. Informed consent was given by the parents and approval by the local ethics committee. After density gradient centrifugation, CD34^{+} cells were enriched by magnetic beads. Purity of cells was evaluated by flow cytometry and generally >90%. Isolated cells were cultured in serum-free medium supplemented with ES-FBS (Invitrogen) and the human cytokines SCF and FLT3L (100 ng/ml each), 50 ng/ml TPO, and 20 ng/ml IL-3 (Immunotools or Preprotech). Cells were cultured at a density of 10^5–10^6/ml. Alternatively, purified cells were frozen in serum/10% DMSO, stored in liquid nitrogen, and used at later time points.

Adenoviral vectors

Recombinant plasmids were generated using Gateway cloning technology (Invitrogen) based on the pAd/CMV/V5-DEST vector (Invitrogen). Because of deletions in the E1 and E3 genes, the viruses were replication incompetent. For adenoviral generation and amplification, a protocol from Luo et al. (2007) was adapted. In brief, HEK293A cells were transfected at a confluence of ∼50–70% using the ProFection Mammalian Transfection System (Promega) according to manufacturer's recommendations. When cell lysis became evident, cells were scraped off and viral release was promoted by four freeze–thaw–vortex cycles. Viruses were stepwise amplified three more times by adding the viral supernatant to increasing HEK293A cell numbers. Viral supernatant was purified using the Vivapure AdenoPACK kit (Sartorius) according to manufacturer's recommendations. For transduction, LSK cells and viruses were coincubated at 37°C for 4 h at a multiplicity of infection of 10 in medium. Venus and BCL-XL overexpression was confirmed by Western blotting or flow cytometry. Adenoviral work was approved by the

local committees (RP Tübingen/Germany) and performed under S2 safety conditions.

TAT–BH4 peptide and TAT–Bcl-xL protein

TAT-BH4 was purchased from Merck or Genaxxon, and FITC-TAT-BH4 was obtained from Genaxxon. The plasmid expressing TAT–Bcl-xL was cloned into the pTAT-HA vector (generated by S. Dowdy) by G. Dietz, who made it available for this study (Dietz et al., 2002). Human TAT–BCL-XL was also cloned into the pTAT-HA vector generated by S. Dowdy. The expression cassette also included a sequence encoding six histidine residues and an HA sequence. Expression and purification of mouse TAT–Bcl-xL and human TAT–BCL-XL was performed as described previously (Dietz and Bahr, 2007). In brief, BL21(DE3)-RIPL *Escherichia coli* were transformed with pTAT–Bcl-xL and amplified in ampicillin– and chloramphenicol-containing LB media, and protein expression was induced by thiogalactopyranoside. Proteins were extracted using an EmulsiFlex-C5 (Avestin). The supernatant was subjected to metal-affinity chromatography using Ni-NTA (Qiagen). For salt/denaturant removal and buffer exchange, affinity-purified proteins were added to PD-10 columns (GE Healthcare Life Sciences) and eluted with a buffer containing 10 mM Tris, pH 10, 0.1 mM EDTA, 15% glycerol, 0.1% pluronic acid, and 0.02% Tween-80. The identity of the protein was confirmed by Western blotting.

To facilitate peptide or protein transduction, mouse LSK cells or human CD34$^+$ cells cultured in whole medium were first treated with 100 µg/ml dextran sulfate for 30 min and subsequently incubated with 500–2,000 nM TAT-BH4 for 12 h or 1.5 µM TAT–Bcl-xL for 2 h. To increase protein uptake in human CD34$^+$ cells, cells were also treated with 5 mM methyl–β-cyclodextrin (Sigma) for 30 min, with or without dextran sulfate. In addition, we analyzed the influence of different temperatures (4°C, 30°C, and 37°C) on protein transduction efficiency (Fretz et al., 2007). The Chariot reagent (Active Motif) was used according to the manufacturer's protocol with β-galactosidase as positive control. In addition, we used the protocol of repeated protein transduction reported by Krosl et al. (2003).

Transplantation assays

For competitive reconstitution assays, 30,000 adenovirally transduced Ly5.1$^+$ LSK cells and 30,000 adenovirally transduced Ly5.2$^+$ LSK cells were mixed and transplanted intravenously into Ly5.1/Ly5.2 heterozygous C57BL/6 mice that were lethally irradiated (9.5 Gy) 6–8 h earlier. When *Rag1$^{-/-}$* mice were used as recipients, 20,000 Ly5.1$^+$ and 20,000 Ly5.2$^+$ cells were used for transplantation. When TAT–Bcl-xL protein transduction was used to influence transplantation outcome, 20,000 Ly5.1$^+$ and 20,000 Ly5.2$^+$ LSK cells were used for competitive transplantation. At indicated time points, recipient mice were sacrificed and hematological organs were analyzed by flow cytometry. Another set of Ly5.1$^+$ recipient mice was transplanted with 15,000 Ly5.2$^+$ LSK cells

transduced with Ad5-Venus or Ad5–BCL-XL, together with 200,000 untreated Ly5.1$^+$ whole BM cells and analyzed 1 yr after transplantation. BM from these animals was used for serial transplantation, and secondary recipients were analyzed 16 wk later. When Eµ-*MYC* transgenic mice were used as donors, 20,000 differentially treated Eµ-*MYC* tg LSK cells were transplanted, and 200,000 Eµ-myc total BM cells were cotransplanted to ensure mouse survival. Recipient mice were closely monitored for lymphoma development and sacrificed when in poor general condition.

Clonogenicity assay

Colony-forming assays were performed by plating 300 LSK cells on a semisolid medium containing insulin, transferrin, rmSCF, rmIL-3, rhIL-6, and rhEPO (GF M3434; Metho-Cult). After incubating cells for 7 d at 37°C, the different colony types were quantified by light microscopy based on typical morphological features.

Flow cytometric analysis

Single-cell suspensions of hematopoietic organs were surface stained with monoclonal antibodies conjugated with FITC, PE, APC, PE-Cy7, or biotin. The antibodies used for mouse cell-surface markers were anti-CD11b (M1/70), anti–Ly-6G/Ly-6C (RB6-8C5), anti–CD45R/B220 (RA3-6B2), anti–IgM (RMM-1), anti-CD4 (RM4-5), anti-CD8a (53–6.7), anti-CD45.1 (A20), anti-CD45.2 (104), anti-CD117 (2B8/3C11), anti–Ly-6A/E (D7/E13-161.7), anti–TER-119 (TER119), anti-CD44 (IM7), and anti-CD25 (PC61); all were purchased from eBioscience or BioLegend. The lineage cocktail (eBioscience) contained the following antibodies: anti-CD11b (Mac-1) M1/70, anti–CD3e 145-2C11, anti–CD45R (B220) RA3-6B2, anti–Ly6G (Gr-1) RB6-8C5, anti–TER-119 Ly-76, and anti–Nk1.1 PK136. Antibodies for human cell surface markers were anti-CD45 (HI30 and 30-F11) and anti-CD34 (AC136). For mouse TAT–Bcl-xL and human TAT–BCL-XL detection by intracellular flow cytometry, cells were fixed using 4% paraformaldehyde, permeabilized with PBS/0.5% saponin, and stained with anti–Bcl-xL (H-5) mouse mAb (Santa Cruz Biotechnology) in PBS/0.5% saponin for 30 min. Biotinylated antibodies were detected using streptavidin coupled to PE or PE-Cy7. Apoptosis was determined by 7-AAD/Annexin-V stain or the Nicoletti stain (sub-G0) using 7-AAD or DAPI. Flow cytometric analysis was performed using a FACScalibur or a Canto II (BD). Specific apoptosis triggered by cytokine withdrawal or etoposide was calculated by the following equation: (induced apoptosis − spontaneous apoptosis) / (100 − spontaneous apoptosis).

Immunoblotting

Proteins were purified and size fractioned by 12% SDS-PAGE under reducing conditions and transferred onto nitrocellulose membranes by electroblotting. For detection of TAT–Bcl-xL, either anti–Bcl-x (44/Bcl-x) mouse mAb (BD Bioscience) or anti–HA-Tag (C29F4) rabbit mAb (Cell Signaling Tech-

nology) was used. As a positive control for BCL-XL over-expression, the Burkitt lymphoma cell line BL40 was used. Secondary reagents were conjugated to peroxidase, and signal was detected by enhanced chemiluminescence. Fractionated Western blotting was performed by using the Mitochondria Isolation kit for Cultured Cells (Thermo Fisher Scientific) according to manufacturer's recommendations.

Immunofluorescence

For fluorescence microscopy, LSK cells were cultured in eight-well μ-Slides (Ibidi), treated with 100 μg/ml dextran sulfate for 30 min, and washed twice with serum-free medium. 1.5 μM Alexa Fluor 488–labeled TAT–Bcl-xL was added for 2 h in serum-free medium. After washing, fresh medium with serum supplemented with 1 μM MitoTracker red and 20 nM Hoechst was added for 15 min. Cells were kept in phenol red–free DMEM at 37°C and 5% CO_2 for imaging using a Zeiss LSM 710 microscope.

Statistical analysis

Statistical analysis was performed using the Mann–Whitney Test (unpaired) or the Wilcoxon test (paired). For survival analysis, the log-rank test (Mantel–Cox test) and Statview 4.1 were used. P-values <0.05 were considered statistically significant. In the figures: *, P < 0.05; **, P < 0.01; ***, P < 0.001.

Online supplemental material

Fig. S1 shows the gating strategy used for analysis of recipient mice. Fig. S2 shows the competitive reconstitution assays using LSK cells infected with adenoviruses. Fig. S3 depicts the in vitro and in vivo experiments using LSK cells treated with Q-VD-OPh and/or Nec1. Fig. S4 depicts the in vitro experiments using LSK cells treated with TAT-BH4. Fig. S5 shows localization and degradation of TAT–BCL-XL protein in HeLa cells.

REFERENCES

Bakanay, Ş.M., and T. Demirer. 2012. Novel agents and approaches for stem cell mobilization in normal donors and patients. *Bone Marrow Transplant.* 47:1154–1163. http://dx.doi.org/10.1038/bmt.2011.170

Ball, L.M., A.C. Lankester, R.G. Bredius, W.E. Fibbe, M.J. van Tol, and R.M. Egeler. 2005. Graft dysfunction and delayed immune reconstitution following haploidentical peripheral blood hematopoietic stem cell transplantation. *Bone Marrow Transplant.* 35:S35–S38. http://dx.doi.org/10.1038/sj.bmt.1704842

Ballen, K.K., E. Gluckman, and H.E. Broxmeyer. 2013. Umbilical cord blood transplantation: The first 25 years and beyond. *Blood.* 122:491–498. http://dx.doi.org/10.1182/blood-2013-02-453175

Barrett, A.J., K. Rezvani, S. Solomon, A.M. Dickinson, X.N. Wang, G. Stark, H. Cullup, M. Jarvis, P.G. Middleton, and N. Chao. 2003. New developments in allotransplant immunology. *Hematology (Am Soc Hematol Educ Program).* 2003:350–371.

Boitano, A.E., J. Wang, R. Romeo, L.C. Bouchez, A.E. Parker, S.E. Sutton, J.R. Walker, C.A. Flaveny, G.H. Perdew, M.S. Denison, et al. 2010. Aryl hydrocarbon receptor antagonists promote the expansion of human hematopoietic stem cells. *Science.* 329:1345–1348. http://dx.doi.org/10.1126/science.1191536

Bradfute, S.B., and M.A. Goodell. 2003. Adenoviral transduction of mouse hematopoietic stem cells. *Mol. Ther.* 7:334–340. http://dx.doi.org/10.1016/S1525-0016(03)00021-2

Butler, J.M., D.J. Nolan, E.L. Vertes, B. Varnum-Finney, H. Kobayashi, A.T. Hooper, M. Seandel, K. Shido, I.A. White, M. Kobayashi, et al. 2010. Endothelial cells are essential for the self-renewal and repopulation of Notch-dependent hematopoietic stem cells. *Cell Stem Cell.* 6:251–264. http://dx.doi.org/10.1016/j.stem.2010.02.001

Chen, B.J., X. Cui, G.D. Sempowski, J. Domen, and N.J. Chao. 2004. Hematopoietic stem cell dose correlates with the speed of immune reconstitution after stem cell transplantation. *Blood.* 103:4344–4352. http://dx.doi.org/10.1182/blood-2003-07-2534

Chen, L., S.N. Willis, A. Wei, B.J. Smith, J.I. Fletcher, M.G. Hinds, P.M. Colman, C.L. Day, J.M. Adams, and D.C. Huang. 2005. Differential targeting of prosurvival Bcl-2 proteins by their BH3-only ligands allows complementary apoptotic function. *Mol. Cell.* 17:393–403. http://dx.doi.org/10.1016/j.molcel.2004.12.030

Czabotar, P.E., G. Lessene, A. Strasser, and J.M. Adams. 2014. Control of apoptosis by the BCL-2 protein family: implications for physiology and therapy. *Nat. Rev. Mol. Cell Biol.* 15:49–63. http://dx.doi.org/10.1038/nrm3722

Delaney, C., S. Heimfeld, C. Brashem-Stein, H. Voorhies, R.L. Manger, and I.D. Bernstein. 2010. Notch-mediated expansion of human cord blood progenitor cells capable of rapid myeloid reconstitution. *Nat. Med.* 16:232–236. http://dx.doi.org/10.1038/nm.2080

de Lima, M., I. McNiece, S.N. Robinson, M. Munsell, M. Eapen, M. Horowitz, A. Alousi, R. Saliba, J.D. McMannis, I. Kaur, et al. 2012. Cord-blood engraftment with ex vivo mesenchymal-cell coculture. *N. Engl. J. Med.* 367:2305–2315. http://dx.doi.org/10.1056/NEJMoa1207285

Dietz, G.P., and M. Bahr. 2007. Synthesis of cell-penetrating peptides and their application in neurobiology. *Methods Mol. Biol.* 399:181–198. http://dx.doi.org/10.1007/978-1-59745-504-6_13

Dietz, G.P., E. Kilic, and M. Bahr. 2002. Inhibition of neuronal apoptosis in vitro and in vivo using TAT-mediated protein transduction. *Mol. Cell. Neurosci.* 21:29–37. http://dx.doi.org/10.1006/mcne.2002.1165

JEM

Donnini, S., R. Solito, M. Monti, W. Balduini, S. Carloni, M. Cimino, E.T. Bampton, L.G. Pinon, P. Nicotera, P.E. Thorpe, and M. Ziche. 2009. Prevention of ischemic brain injury by treatment with the membrane penetrating apoptosis inhibitor, TAT-BH4. *Cell Cycle.* 8:1271–1278. http://dx.doi.org/10.4161/cc.8.8.8301

Edlich, F., S. Banerjee, M. Suzuki, M.M. Cleland, D. Arnoult, C. Wang, A. Neutzner, N. Tjandra, and R.J. Youle. 2011. Bcl-x(L) retrotranslocates Bax from the mitochondria into the cytosol. *Cell.* 145:104–116. http://dx.doi.org/10.1016/j.cell.2011.02.034

Egle, A., A.W. Harris, P. Bouillet, and S. Cory. 2004. Bim is a suppressor of Myc-induced mouse B cell leukemia. *Proc. Natl. Acad. Sci. USA.* 101:6164–6169. http://dx.doi.org/10.1073/pnas.0401471101

Fang, W., J.J. Rivard, D.L. Mueller, and T.W. Behrens. 1994. Cloning and molecular characterization of mouse bcl-x in B and T lymphocytes. *J. Immunol.* 153:4388–4398.

Fretz, M.M., N.A. Penning, S. Al-Taei, S. Futaki, T. Takeuchi, I. Nakase, G. Storm, and A.T. Jones. 2007. Temperature-, concentration- and cholesterol-dependent translocation of L- and D-octa-arginine across the plasma and nuclear membrane of CD34+ leukaemia cells. *Biochem. J.* 403:335–342. http://dx.doi.org/10.1042/BJ20061808

Gerber, H.P., A.K. Malik, G.P. Solar, D. Sherman, X.H. Liang, G. Meng, K. Hong, J.C. Marsters, and N. Ferrara. 2002. VEGF regulates haematopoietic stem cell survival by an internal autocrine loop mechanism. *Nature.* 417:954–958. http://dx.doi.org/10.1038/nature00821

Handgretinger, R., T. Klingebiel, P. Lang, M. Schumm, S. Neu, A. Geiselhart, P. Bader, P.G. Schlegel, J. Greil, D. Stachel, et al. 2001. Megadose transplantation of purified peripheral blood CD34+ progenitor cells from HLA-mismatched parental donors in children. *Bone Marrow Transplant.* 27:777–783. http://dx.doi.org/10.1038/sj.bmt.1702996

Harris, A.W., C.A. Pinkert, M. Crawford, W.Y. Langdon, R.L. Brinster, and J.M. Adams. 1988. The E mu-myc transgenic mouse. A model for high-incidence spontaneous lymphoma and leukemia of early B cells. *J. Exp. Med.* 167:353–371. http://dx.doi.org/10.1084/jem.167.2.353

Haspel, R.L., and K.K. Ballen. 2006. Double cord blood transplants: Filling a niche? *Stem Cell Rev.* 2:81–86.

Hooper, A.T., J.M. Butler, D.J. Nolan, A. Kranz, K. Iida, M. Kobayashi, H.G. Kopp, K. Shido, I. Petit, K. Yanger, et al. 2009. Engraftment and reconstitution of hematopoiesis is dependent on VEGFR2-mediated regeneration of sinusoidal endothelial cells. *Cell Stem Cell.* 4:263–274. http://dx.doi.org/10.1016/j.stem.2009.01.006

Horwitz, M.E. 2016. Ex vivo expansion or manipulation of stem cells to improve outcome of umbilical cord blood transplantation. *Curr. Hematol. Malig. Rep.* 11:12–18. http://dx.doi.org/10.1007/s11899-015-0297-7

Hotchkiss, R.S., K.W. McConnell, K. Bullok, C.G. Davis, K.C. Chang, S.J. Schwulst, J.C. Dunne, G.P. Dietz, M. Bahr, J.E. McDunn, et al. 2006. TAT-BH4 and TAT-Bcl-xL peptides protect against sepsis-induced lymphocyte apoptosis in vivo. *J. Immunol.* 176:5471–5477. http://dx.doi.org/10.4049/jimmunol.176.9.5471

Huang, D.C., J.M. Adams, and S. Cory. 1998. The conserved N-terminal BH4 domain of Bcl-2 homologues is essential for inhibition of apoptosis and interaction with CED-4. *EMBO J.* 17:1029–1039. http://dx.doi.org/10.1093/emboj/17.4.1029

Klein, D., M.M. Ribeiro, V. Mendoza, S. Jayaraman, N.S. Kenyon, A. Pileggi, R.D. Molano, L. Inverardi, C. Ricordi, and R.L. Pastori. 2004. Delivery of Bcl-XL or its BH4 domain by protein transduction inhibits apoptosis in human islets. *Biochem. Biophys. Res. Commun.* 323:473–478. http://dx.doi.org/10.1016/j.bbrc.2004.08.116

Kollek, M., A. Muller, A. Egle, and M. Erlacher. 2016. Bcl-2 proteins in development, health and disease of the hematopoietic system. *FEBS J.* 283:2779–2810. http://dx.doi.org/10.1111/febs.13683

Krosl, J., P. Austin, N. Beslu, E. Kroon, R.K. Humphries, and G. Sauvageau. 2003. In vitro expansion of hematopoietic stem cells by recombinant TAT-HOXB4 protein. *Nat. Med.* 9:1428–1432. http://dx.doi.org/10.1038/nm951

Labi, V., M. Erlacher, S. Kiessling, and A. Villunger. 2006. BH3-only proteins in cell death initiation, malignant disease and anticancer therapy. *Cell Death Differ.* 13:1325–1338. http://dx.doi.org/10.1038/sj.cdd.4401940

Labi, V., D. Bertele, C. Woess, D. Tischner, F.J. Bock, S. Schwemmers, H.L. Pahl, S. Geley, M. Kunze, C.M. Niemeyer, et al. 2013. Haematopoietic stem cell survival and transplantation efficacy is limited by the BH3-only proteins Bim and Bmf. *EMBO Mol. Med.* 5:122–136. http://dx.doi.org/10.1002/emmm.201201235

Labi, V., C. Woess, S. Tuzlak, M. Erlacher, P. Bouillet, A. Strasser, A. Tzankov, and A. Villunger. 2014. Deregulated cell death and lymphocyte homeostasis cause premature lethality in mice lacking the BH3-only proteins Bim and Bmf. *Blood.* 123:2652–2662. http://dx.doi.org/10.1182/blood-2013-11-537217

Luo, J., Z.L. Deng, X. Luo, N. Tang, W.X. Song, J. Chen, K.A. Sharff, H.H. Luu, R.C. Haydon, K.W. Kinzler, et al. 2007. A protocol for rapid generation of recombinant adenoviruses using the AdEasy system. *Nat. Protoc.* 2:1236–1247. http://dx.doi.org/10.1038/nprot.2007.135

Maie, K., S. Fuji, K. Tajima, M. Tatsuno, S. Yamagata, N. Takahashi, R. Ueda, H. Hashimoto, K. Takano, Y. Inoue, et al. 2014. A higher number of infused CD34+ cells has a positive impact on the clinical outcome after related PBSC transplantation. *Bone Marrow Transplant.* 49:1113–1115. http://dx.doi.org/10.1038/bmt.2014.94

Mattsson, J., O. Ringden, and R. Storb. 2008. Graft failure after allogeneic hematopoietic cell transplantation. *Biol. Blood Marrow Transplant.* 14:165–170. http://dx.doi.org/10.1016/j.bbmt.2007.10.025

McConnell, M.J., and M.J. Imperiale. 2004. Biology of adenovirus and its use as a vector for gene therapy. *Hum. Gene Ther.* 15:1022–1033. http://dx.doi.org/10.1089/hum.2004.15.1022

Mogul, M.J. 2000. Unrelated cord blood transplantation vs matched unrelated donor bone marrow transplantation: The risks and benefits of each choice. *Bone Marrow Transplant.* 25:S58–S60. http://dx.doi.org/10.1038/sj.bmt.1702372

Mombaerts, P., J. Iacomini, R.S. Johnson, K. Herrup, S. Tonegawa, and V.E. Papaioannou. 1992. RAG-1-deficient mice have no mature B and T lymphocytes. *Cell.* 68:869–877. http://dx.doi.org/10.1016/0092-8674(92)90030-G

Monaco, G., E. Decrock, N. Arbel, A.R. van Vliet, R.M. La Rovere, S.H. De, J.B. Parys, P. Agostinis, L. Leybaert, V. Shoshan-Barmatz, and G. Bultynck. 2015. The BH4 domain of anti-apoptotic Bcl-XL, but not that of the related Bcl-2, limits the voltage-dependent anion channel 1 (VDAC1)-mediated transfer of pro-apoptotic Ca2+ signals to mitochondria. *J. Biol. Chem.* 290:9150–9161. http://dx.doi.org/10.1074/jbc.M114.622514

Murray, L.J., J.C. Young, L.J. Osborne, K.M. Luens, R. Scollay, and B.L. Hill. 1999. Thrombopoietin, flt3, and kit ligands together suppress apoptosis of human mobilized CD34+ cells and recruit primitive CD34+ Thy-1+ cells into rapid division. *Exp. Hematol.* 27:1019–1028. http://dx.doi.org/10.1016/S0301-472X(99)00031-4

Purton, L.E., and D.T. Scadden. 2007. Limiting factors in murine hematopoietic stem cell assays. *Cell Stem Cell.* 1:263–270. http://dx.doi.org/10.1016/j.stem.2007.08.016

Puthalakath, H., A. Villunger, L.A. O'Reilly, J.G. Beaumont, L. Coultas, R.E. Cheney, D.C. Huang, and A. Strasser. 2001. Bmf: A proapoptotic BH3-only protein regulated by interaction with the myosin V actin motor complex, activated by anoikis. *Science.* 293:1829–1832. http://dx.doi.org/10.1126/science.1062257

Reissmann, S. 2014. Cell penetration: Scope and limitations by the application of cell-penetrating peptides. *J. Pept. Sci.* 20:760–784. http://dx.doi.org/10.1002/psc.2672

Rocha, V., and H.E. Broxmeyer. 2010. New approaches for improving engraftment after cord blood transplantation. *Biol. Blood Marrow Transplant.* 16:S126–S132. http://dx.doi.org/10.1016/j.bbmt.2009.11.001

Sehnert, B., H. Burkhardt, S. Dubel, and R.E. Voll. 2015. The "sneaking-ligand" approach: Cell-type specific inhibition of the classical NF-κB pathway. *Methods Mol. Biol.* 1280:559–578. http://dx.doi.org/10.1007/978-1-4939-2422-6_33

Shen, H., J.C. Mai, L. Qiu, S. Cao, P.D. Robbins, and T. Cheng. 2004. Evaluation of peptide-mediated transduction in human CD34+ cells. *Hum. Gene Ther.* 15:415–419. http://dx.doi.org/10.1089/104303404322959560

Stephen, S.L., E. Montini, V.G. Sivanandam, M. Al-Dhalimy, H.A. Kestler, M. Finegold, M. Grompe, and S. Kochanek. 2010. Chromosomal integration of adenoviral vector DNA in vivo. *J. Virol.* 84:9987–9994. http://dx.doi.org/10.1128/JVI.00751-10

Strasser, A., A.W. Harris, M.L. Bath, and S. Cory. 1990. Novel primitive lymphoid tumours induced in transgenic mice by cooperation between myc and bcl-2. *Nature.* 348:331–333. http://dx.doi.org/10.1038/348331a0

Sugioka, R., S. Shimizu, T. Funatsu, H. Tamagawa, Y. Sawa, T. Kawakami, and Y. Tsujimoto. 2003. BH4-domain peptide from Bcl-xL exerts anti-apoptotic activity in vivo. *Oncogene.* 22:8432–8440. http://dx.doi.org/10.1038/sj.onc.1207180

Varnum-Finney, B., L. Xu, C. Brashem-Stein, C. Nourigat, D. Flowers, S. Bakkour, W.S. Pear, and I.D. Bernstein. 2000. Pluripotent, cytokine-dependent, hematopoietic stem cells are immortalized by constitutive Notch1 signaling. *Nat. Med.* 6:1278–1281. http://dx.doi.org/10.1038/81390

Villunger, A., C. Scott, P. Bouillet, and A. Strasser. 2003. Essential role for the BH3-only protein Bim but redundant roles for Bax, Bcl-2, and Bcl-w in the control of granulocyte survival. *Blood.* 101:2393–2400. http://dx.doi.org/10.1182/blood-2002-07-2132

Wagner, J.E., J.N. Barker, T.E. DeFor, K.S. Baker, B.R. Blazar, C. Eide, A. Goldman, J. Kersey, W. Krivit, M.L. MacMillan, et al. 2002. Transplantation of unrelated donor umbilical cord blood in 102 patients with malignant and nonmalignant diseases: Influence of CD34 cell dose and HLA disparity on treatment-related mortality and survival. *Blood.* 100:1611–1618.

Wagner, J.E. Jr., C.G. Brunstein, A.E. Boitano, T.E. DeFor, D. McKenna, D. Sumstad, B.R. Blazar, J. Tolar, C. Le, J. Jones, et al. 2016. Phase I/II trial of StemRegenin-1 expanded umbilical cord blood hematopoietic stem cells supports testing as a stand-alone graft. *Cell Stem Cell.* 18:144–155. http://dx.doi.org/10.1016/j.stem.2015.10.004

Waterstrat, A., Y. Liang, C.F. Swiderski, B.J. Shelton, and Z.G. Van. 2010. Congenic interval of CD45/Ly-5 congenic mice contains multiple genes that may influence hematopoietic stem cell engraftment. *Blood.* 115:408–417. http://dx.doi.org/10.1182/blood-2008-03-143370

White, M.J., K. McArthur, D. Metcalf, R.M. Lane, J.C. Cambier, M.J. Herold, M.F. van Delft, G. Lessene, M.E. Ritchie, et al. 2014. Apoptotic caspases suppress mtDNA-induced STING-mediated type I IFN production. *Cell.* 159:1549–1562. http://dx.doi.org/10.1016/j.cell.2014.11.036

Woess, C., S. Tuzlak, V. Labi, M. Drach, D. Bertele, P. Schneider, and A. Villunger. 2015. Combined loss of the BH3-only proteins Bim and Bmf restores B-cell development and function in TACI-Ig transgenic mice. *Cell Death Differ.* 22:1477–1488. http://dx.doi.org/10.1038/cdd.2015.8

Yabe, M., T. Morimoto, T. Shimizu, T. Koike, H. Takakura, K. Ohtsubo, A. Fukumura, S. Kato, and H. Yabe. 2014. Feasibility of marrow harvesting from pediatric sibling donors without hematopoietic growth factors and allotransfusion. *Bone Marrow Transplant.* 49:921–926. http://dx.doi.org/10.1038/bmt.2014.73